4-1-2017

Rapid and rigorous IL-17A production by a distinct subpopulation of effector memory T lymphocytes constitutes a novel mechanism of toxic shock syndrome immunopathology

Peter A. Szabo
The University of Western Ontario

Ankur Goswami
The University of Western Ontario

Delfina M. Mazzuca
The University of Western Ontario

Kyoungok Kim
The University of Western Ontario

David B. O'Gorman
Hand and Upper Limb Centre

See next page for additional authors

Rapid and Rigorous IL-17A Production by a Distinct Subpopulation of Effector Memory T Lymphocytes Constitutes a Novel Mechanism of Toxic Shock Syndrome Immunopathology

Peter A. Szabo,* Ankur Goswami,* Delfina M. Mazzuca,* Kyoungok Kim,* David B. O'Gorman,[†,‡,§,¶] David A. Hess,[‖,#] Ian D. Welch, Howard A. Young,[††] Bhagirath Singh,[*,§,‡‡] John K. McCormick,[*,§,‡‡] and S. M. Mansour Haeryfar[*,§,‡‡,§§]**

Toxic shock syndrome (TSS) is caused by staphylococcal and streptococcal superantigens (SAgs) that provoke a swift hyperinflammatory response typified by a cytokine storm. The precipitous decline in the host's clinical status and the lack of targeted therapies for TSS emphasize the need to identify key players of the storm's initial wave. Using a humanized mouse model of TSS and human cells, we herein demonstrate that SAgs elicit in vitro and in vivo IL-17A responses within hours. SAg-triggered human IL-17A production was characterized by remarkably high mRNA stability for this cytokine. A distinct subpopulation of $CD4^+$ effector memory T (T_{EM}) cells that secrete IL-17A, but not IFN-γ, was responsible for early IL-17A production. We found mouse "T_{EM}-17" cells to be enriched within the intestinal epithelium and among lamina propria lymphocytes. Furthermore, interfering with IL-17A receptor signaling in human PBMCs attenuated the expression of numerous inflammatory mediators implicated in the TSS-associated cytokine storm. IL-17A receptor blockade also abrogated the secondary effect of SAg-stimulated PBMCs on human dermal fibroblasts as judged by C/EBP δ expression. Finally, the early IL-17A response to SAgs was pathogenic because in vivo neutralization of IL-17A in humanized mice ameliorated hepatic and intestinal damage and reduced mortality. Together, our findings identify $CD4^+$ T_{EM} cells as a key effector of TSS and reveal a novel role for IL-17A in TSS immunopathogenesis. Our work thus elucidates a pathogenic, as opposed to protective, role for IL-17A during Gram-positive bacterial infections. Accordingly, the IL-17–IL-17R axis may provide an attractive target for the management of SAg-mediated illnesses. ***The Journal of Immunology*****, 2017, 198: 2805–2818.**

Toxic shock syndrome (TSS) is a life-threatening illness characterized by high-grade fever, diffuse erythematous rash formation, desquamation, severe hypotension, and multiorgan dysfunction (1). It is caused by systemic exposure to bacterial toxins known as superantigens (SAgs), which are secreted by *Staphylococcus aureus* and *Streptococcus pyogenes*. TSS can be of menstrual (2) or nonmenstrual (3) origin. The vast majority of menstrual TSS cases, which are linked to high-absorbency tampon usage (4), are caused by *S. aureus* strains expressing the powerful SAg TSS toxin-1 (TSST-1) (5). In contrast, nonmenstrual TSS can occur with virtually any *S. aureus* infection and is primarily associated with TSST-1 and staphylococcal enterotoxin B (SEB) (6). The expression of streptococcal pyrogenic exotoxin A (SpeA) is also strongly correlated with streptococcal TSS (7).

SAgs are a unique family of exotoxins that activate a large proportion of T cells irrespective of their TCR specificity. Cognate peptide Ags presented in the context of self-MHC by APCs typically activate one in every 10,000 T cells. In contrast, SAgs simultaneously bind MHC class II molecules on APCs outside their Ag-binding groove (8) and select TCR Vβ domains on T cells (9). By doing so, SAgs circumvent conventional modes of Ag processing and presentation to induce the activation and proliferation of up to 50% of all exposed T cells (10). The overwhelming activation of T cells by SAgs results in excessive production of inflammatory mediators, which is commonly referred to as cytokine

*Department of Microbiology and Immunology, Western University, London, Ontario N6A 5C1, Canada; [†]Cell and Molecular Biology Laboratory, Roth | McFarlane Hand and Upper Limb Centre, Western University, London, Ontario N6A 4V2, Canada; [‡]Department of Biochemistry, Western University, London, Ontario N6A 5C1, Canada; [§]Lawson Health Research Institute, London, Ontario N6C 2R5, Canada; [¶]Department of Surgery, Western University, London, Ontario N6A 4V2, Canada; [‖]Department of Physiology and Pharmacology, Western University, London, Ontario N6A 5C1, Canada; [#]Krembil Centre for Stem Cell Biology, Molecular Medicine Research Group, Robarts Research Institute, London, Ontario N6A 5B7, Canada; **Department of Pathology and Laboratory Medicine, University of British Columbia, Vancouver, British Columbia V6T 2B5, Canada; [††]Cancer and Inflammation Program, Center for Cancer Research, National Cancer Institute-Frederick, Frederick, MD 21702; [‡‡]Centre for Human Immunology, Western University, London, Ontario N6A 5C1, Canada; and [§§]Division of Clinical Immunology and Allergy, Department of Medicine, Western University, London, Ontario N6A 5A5, Canada

ORCIDs: 0000-0001-6195-2644 (D.B.O.); 0000-0002-3118-5111 (H.A.Y.); 0000-0002-9792-8694 (B.S.); 0000-0003-3742-7289 (J.K.M.); 0000-0002-1125-8176 (S.M.M.H.).

Received for publication August 5, 2016. Accepted for publication January 25, 2017.

This work was supported by a Canadian Institutes of Health Research operating grant (Grant MOP-130465) to S.M.M.H.

Address correspondence and reprint requests to Dr. S. M. Mansour Haeryfar, Western University, Room SDRI 234, 1151 Richmond Street, London, ON N6A 5C1, Canada. E-mail address: Mansour.Haeryfar@schulich.uwo.ca

The online version of this article contains supplemental material.

Abbreviations used in this article: act-D, actinomycin D; CEBPD, C/EBP δ; C_T, cycle threshold; D17, HLA-DR4 transgenic IL-17A reporter; DR4tg, HLA-DR4 transgenic; IEL, intraepithelial lymphocyte; IL-17RA, IL-17 receptor A; *i*NKT, invariant NKT; LPL, lamina propria lymphocyte; MAIT, mucosa-associated invariant T; MFI, mean fluorescence intensity; qPCR, quantitative real-time PCR; RPL13A, ribosomal protein L13a; SAg, superantigen; SEA, staphylococcal enterotoxin A; SEB, staphylococcal enterotoxin B; SmeZ, streptococcal mitogenic exotoxin Z; SpeA, streptococcal pyrogenic exotoxin A; SpeI, streptococcal pyrogenic exotoxin I; T_{EM}, effector memory T; TSS, toxic shock syndrome; TSST-1, TSS toxin-1.

www.jimmunol.org/cgi/doi/10.4049/jimmunol.1601366

storm. SAgs directly stimulate the secretion of IL-2, IFN-γ, and lymphotoxin-α from T cells, as well as TNF-α, IL-1β, and IL-6 from APCs (10, 11). Additionally, SAgs initiate secondary inflammatory cytokine and chemokine responses from various nonhematopoietic cell types such as epithelial cells, endothelial cells, and fibroblasts (12). The massive and uncontrolled release of these inflammatory mediators has drastic tissue damaging effects through the activation of the coagulatory cascade, vasodilation, edema, and vascular leakage (13–16). SAgs also promote the production of chemokines CXCL8, CCL2, CCL3, and CCL4 (17, 18), resulting in further recruitment of leukocytes to areas of tissue injury. The net effect of the cytokine storm is a systemic inflammatory response syndrome that may culminate in fatal multiorgan failure.

IL-17A is a potent inducer of systemic inflammation, potentiating the production or activation of inflammatory cytokines (e.g., TNF-α, IL-1β, and IL-6), chemokines, matrix metalloproteases, and transcription factors in both hematopoietic and nonhematopoietic cell types (19). IL-17A also acts synergistically with other inflammatory cytokines, including TNF-α, IL-1β, and IFN-γ, to stabilize mRNA transcripts or activate promoter regions of other inflammatory mediators (20). Although IL-17A is the archetypal cytokine of the $CD4^+$ Th17 cell lineage (19), it can also be quickly produced by innate-like T lymphocytes such as γδ T cells, invariant NKT (*i*NKT) cells, and mucosa-associated invariant T (MAIT) cells (21, 22). IL-17A is often associated with early and protective host responses to bacteria, and little is known about its pathogenic potentials during infection. For example, whether exposure to SAgs elicits an early IL-17A response that may contribute to the cytokine storm is essentially unexplored.

Identification of early inflammatory mediators of the cytokine storm and their cellular sources is of utmost importance due to the rapidity with which TSS may progress to life-threatening disease. The clinical status of a SAg-exposed individual can deteriorate to multiorgan failure as early as 8–12 h after the onset of the symptoms (23), and estimates of TSS mortality range from 4 to 22% (24–26). Also alarmingly, there are currently no available therapeutics to attenuate the cytokine storm, which drives the immunopathology of TSS. Therefore, understanding the critical components of this process may hold the key to designing effective therapies that reduce TSS-associated morbidity and mortality.

In this investigation, using humanized mice and human PBMCs, we found and characterized a vigorous IL-17A response that was detectable within the first few hours of SAg exposure. The kinetics of this response initially suggested the involvement of innate-like T cells (21), which we were able to rule out. Instead, we identified effector memory T (T_{EM}) cells as the major source of mouse and human IL-17A, which were surprisingly unable to coproduce IFN-γ. IL-17A receptor blockade diminished the expression of several proinflammatory mediators by SAg-stimulated human PBMCs and also prevented the secondary upregulation of the transcription factor C/EBP δ (CEBPD) in human dermal fibroblasts. These findings suggested a pathogenic role for IL-17A in TSS, which we confirmed using a humanized mouse model of the syndrome. Therefore, to our knowledge, this work defines a previously unrecognized mechanism of TSS immunopathology that is dependent upon rapid IL-17A production by a distinct subpopulation of T_{EM} cells.

Materials and Methods

Mice

Adult 6–12 wk-old mice closely matched for age and sex were used in all experiments. Wild-type C57BL/6 mice were purchased from Charles River Canada (Saint-Constant, QC). IL-17A–GFP mice that express enhanced GFP as a marker of IL-17A expression were obtained from The Jackson Laboratory (Bar Harbor, ME) and bred in a barrier facility at Western University. HLA-DR4 transgenic (DR4tg) mice, which are devoid of endogenous MHC class II and instead express HLA-DRA-IEα and HLA-DRB1*0401-IEβ on a C57BL/6 background (27), were bred in the same facility.

To develop a SAg-sensitive IL-17A reporter mouse strain, DR4tg and IL-17A–GFP mice were crossed. The resultant HLA-DR4 transgenic IL-17A reporter (D17) mice were bred to homozygosity and confirmed to express HLA-DR transgenes and the IL-17A–GFP reporter construct but not IAβ. In brief, genomic DNA was extracted from mouse ear clips using hot sodium hydroxide and Tris. PCR-amplified products were generated using Platinum Taq DNA polymerase (Thermo Fisher Scientific, Ottawa, ON) and primer sets that are listed in Supplemental Table I. Agarose gel electrophoresis was performed to visualize PCR products.

Wild-type C57BL/6, IL-17A–GFP, DR4tg, and D17 mice were cared for in the same facility. All animal experiments were conducted in accordance with an approved institutional animal use protocol (AUP 2010-241) and in compliance with the Canadian Council on Animal Care guidelines.

Generation of bone marrow chimeras

To obtain donor cells, IL-17A–GFP mice were euthanized by cervical dislocation, and bone marrow was flushed out of femurs and tibias with ice-cold PBS. Erythrocytes were lysed by addition of ACK lysis buffer for 2 min, and resulting cells were filtered through a 70-μm nylon mesh strainer. Twenty million donor cells were injected i.v. into recipient DR4tg mice, which were lethally irradiated at 9 Gy using a [^{137}Cs] gamma irradiator before adoptive transfer. Recipient mice were maintained on drinking water supplemented with 2 mg/ml neomycin sulfate (Teknova, Hollister, CA) for 2 wk after irradiation to prevent infection.

Bacterial toxins

Recombinant staphylococcal and streptococcal SAgs were generated using an approved institutional biosafety protocol that follows established Public Health Agency of Canada regulations as described previously (28). Briefly, SAgs were expressed in BL21 (DE3) *Escherichia coli* and purified by nickel column chromatography. As an additional control, an attenuated mutant of SEB that is impaired in binding to mouse TCR Vβ8.2 (29) was generated by site-directed mutagenesis (30). The mutant SEB carries an N→A point mutation at position 23 and is referred to as SEB_{N23A}. LPS was purchased from Sigma-Aldrich (Oakville, ON).

Toxic shock syndrome mouse model and in vivo IL-17A neutralization

Animals were injected i.p. with indicated amounts of SEB or the equivalent volume of PBS as a control. They were bled via the saphenous vein, and serum samples were obtained following centrifugation of blood at 17,000 × *g* for 40 min and analyzed for their cytokine content using ELISA kits from eBioscience (San Diego, CA). For in vivo IL-17A neutralization, DR4tg mice were treated with 200-μg i.p. doses of an anti–IL-17A mAb (clone 17F3; BioXCell, West Lebanon, NH) or a mouse IgG1 isotype control (clone MOPC-21) 3 h before and 1 h after they were injected with 100 μg SEB. Mice were monitored every 3 h for the initial 12 h and every 8 h thereafter for up to 7 d. Weight loss was assessed at indicated time points, and mice were sacrificed when 20% weight loss was reached following institutional protocols and Canadian Council on Animal Care guidelines. For histological analyses, mice were sacrificed at 48 h post-SEB stimulation. Liver and small intestine were extracted, fixed in 10% neutral-buffered formalin, embedded in paraffin, sectioned, and stained with H&E. Sections were scored by a board-certified veterinary pathologist who was blinded to the experimental conditions.

Human PBMC isolation and stimulation with SAgs

Peripheral blood was collected in heparinized vacutainers from healthy volunteers after their written consent was secured and following a protocol approved by the Western University Research Ethics Board for Health Sciences Research Involving Human Subjects (HSREB 5545). PBMCs were isolated by density centrifugation using 50-ml SepMate tubes from Stemcell Technologies (Vancouver, BC) and low endotoxin (<0.12 endotoxin units per ml) Ficoll-Paque Plus (GE Healthcare Life Sciences) according to the manufacturer's instructions. PBMCs were suspended in RPMI 1640 medium supplemented with 10% heat-inactivated FCS, 0.1 mM MEM nonessential amino acids, 2 mM GlutaMAX-I, 1 mM sodium pyruvate, 10 mM HEPES, 100 U/ml penicillin and 100 μg/ml

streptomycin. PBMCs were stimulated with 100 ng/ml of indicated SAgs for up to 24 h at 37°C in polystyrene U-bottom plates at a density of 2×10^6 per well. To block IL-17 receptor A (IL-17RA) prior to SEB stimulation, PBMCs were incubated with 10 μg/ml of an anti–IL-17RA mAb (clone 133617) or mouse IgG1 isotype control (clone 11711) from R&D Systems (Minneapolis, MN) for 30 min.

For cytokine assays, culture supernatants were harvested at indicated time points and analyzed by a bead-based multiplex assay (Eve Technologies, Calgary, AB). Heat maps were generated using the matrix2png utility (31). For RNA studies, PBMCs were isolated in RNAlater (Thermo Fisher Scientific) and RNA was extracted using the Purelink RNA Mini Kit (Thermo Fisher Scientific). To eliminate contaminating genomic DNA, on-column Purelink DNase (Invitrogen Canada, Burlington, ON) was used as per the manufacturer's instructions. RNA quantity and purity was measured by a NanoDrop ND-1000 spectrophotometer. RNA was converted to cDNA via SuperScript VILO Master Mix (Invitrogen Canada). Quantitative real-time PCR (qPCR) was performed on a StepOnePlus Real-Time PCR System using TaqMan Gene Expression Assays (Supplemental Table II) and TaqMan Fast Advanced Master Mix, all from Thermo Fisher Scientific. qPCR reactions and cycling conditions were set up according to the manufacturer's instructions. Fold changes between conditions were calculated by the ΔΔ cycle threshold (C_T) method. For low-expressing gene targets that consistently amplified with C_T values >37, C_T values were set to 37 for analysis.

As reliable comparisons of gene expression by qPCR require normalization to stably expressed reference genes, we first tested several commonly used reference genes for changes in SEB-stimulated PBMCs when compared with unstimulated controls. The mean fold changes of TATA-binding protein and ribosomal protein L13a (RPL13A) were no more or less than 20% (data not shown). TATA-binding protein and/or RPL13A were thus used as reference genes in our qPCR assays.

To analyze RNA stability/degradation, PBMCs were stimulated with SEB for 4 h followed by treatment with 5 μg/ml transcriptional inhibitor actinomycin D (act-D). Cells were harvested at indicated time points, RNA was extracted and converted to cDNA, and qPCR for target genes was performed as described above using 18S RNA as the reference gene.

Human PBMC-dermal fibroblast coculturing

Using an approved ethics protocol (HSREB 104888), primary human fibroblasts were derived from surgically resected normal skin samples as previously described (32). Fibroblast cultures were maintained for a maximum of six passages in DMEM medium containing 10% heat-inactivated FCS, 2 mM GlutaMAX-I and 1× Antibiotic-Antimycotic (Thermo Fisher Scientific). Fibroblasts were seeded at a density of 5×10^5 per well in a tissue culture–treated polystyrene flat-bottom plate. Four million freshly isolated PBMCs were plated into a Nunc Polycarbonate Membrane Insert (pore size: 0.4 μm), which was placed inside the fibroblast culture well. Cocultures were then stimulated with 100 ng/ml SEB. Eight hours later, the insert was removed and fibroblasts were harvested and examined by qPCR for their CEBPD expression. In several experiments, anti–IL-17RA mAb or isotype control was added to cocultures at 10 μg/ml 30 min before SEB stimulation.

Isolation and cytofluorimetric analyses of mouse cells

PBS- and SAg-primed mice were sacrificed at indicated time points to harvest spleen, pooled lymph nodes (cervical, axillary, brachial, mesenteric, inguinal, and popliteal nodes), liver, lungs, and small intestine. Spleen and lymph nodes were homogenized using a Wheaton Dounce tissue grinder. To obtain hepatic and lung nonparenchymal mononuclear cells, tissue specimens were pressed through a wire mesh, and the extracted cells were washed, resuspended in 33.75% low endotoxin Percoll Plus (GE Healthcare Life Sciences, Mississauga, ON), and centrifuged at 700 × *g* for 12 min at room temperature. Pelleted cells were treated with ACK lysis buffer, washed, filtered, and resuspended in cold sterile PBS.

Intraepithelial lymphocytes (IELs) and lamina propria lymphocytes (LPLs) were isolated from the small intestine as described by Sheridan and Lefrançois (33). Briefly, the small intestine was aseptically removed, flushed with HBSS containing 5% FCS and 10 mM HEPES, digested at 37°C with 1 mM dithioerythritol, and filtered through a cell strainer (pore size: 70 μm) to generate an IEL-containing homogenate. To prepare LPLs, the remaining intestinal pieces were additionally digested, first in 1.3 mM EDTA and then in a solution containing 100 U/ml collagenase, and subsequently filtered. IEL- and LPL-containing homogenates were washed, resuspended in 44% Percoll Plus (GE Healthcare Life Sciences), underlaid with 67% Percoll Plus, and spun at 600 × *g* for 20 min. IELs and LPLs were harvested by a Pasteur pipette from the buffy coat formed at the gradient interface, washed, and resuspended in cold PBS.

Freshly isolated mouse cells were incubated with 5 μg/ml of an anti-mouse CD16/CD32 mAb (clone 2.4G2) to block Fcγ receptors and stained at 4°C with fluorochrome-conjugated mAbs to cell surface molecules listed in Supplemental Table II. Corresponding isotype controls were used in parallel for appropriate gating. A FACSCanto II cytometer (BD Biosciences, Mississauga, ON) was used for data collection. Data were analyzed by FlowJo software (Tree Star, Ashland, OR).

Surface and intracellular staining of human cells and RNA flow cytometry

Freshly isolated human PBMCs were stimulated with SAgs for 4 h, unless otherwise stated, in the presence of 1 μM brefeldin A (Sigma-Aldrich). Cells were thoroughly washed and stained at 4°C with fluorochrome-conjugated mAbs to cell surface molecules (Supplemental Table II). For intracellular detection of cytokines, the Intracellular Fixation and Permeabilization Buffer Set from eBioscience was used. We also employed a Mouse IL-17A Secretion Assay kit from Miltenyi Biotec (Auburn, CA) to confirm the secretion of this cytokine. For detection of transcription factors, the FoxP3 Staining Buffer Set (eBioscience) was used. For RNA staining, the Prime FlowRNA Assay (eBioscience) was used with probes designed for the detection of IL-17A, IFN-γ and RPL13A signals. Cells were treated and stained for surface and intracellular molecules (Supplemental Table II) following the manufacturer's instructions. Isotype and/or fluorescence minus one controls were used in parallel for proper gating. Samples were run on a BD FACSCanto II or a BD LSR II (when using violet fluorochrome-conjugated mAbs) and analyzed by FlowJo software (Tree Star).

Statistical analyses

Analyses were carried out using GraphPad Prism 7 software (La Jolla, CA). The Shapiro–Wilk test was performed to verify the normal distribution of our data sets. Statistical comparisons were made using parametric Student *t* tests, ANOVA with Holm–Sidak post hoc analysis, or log-rank test, as appropriate and as indicated in the figure legends. Differences with $p \leq 0.05$ were deemed statistically significant.

Results

IL-17A is rapidly produced by CD4$^+$ effector memory T cells in a humanized mouse model of toxic shock syndrome

SAgs have notoriously poor binding affinity for MHC class II molecules expressed in certain conventional mouse strains such as C57BL/6 mice (34). Thus, we investigated the pathogenesis of TSS in humanized DR4tg mice that allow for high-affinity interactions with SAgs and consequently recapitulate many aspects of TSS-mediated immunopathology (28, 29, 35–39). Using this model, we serendipitously found a dramatic serum IL-17A spike at 2 h post-SEB exposure (Fig. 1A). Given that the role of IL-17A in TSS is unknown and that IL-17A induces and synergizes with many inflammatory mediators implicated in the cytokine storm, we sought to fully characterize this phenomenon. IL-17A was present in the serum at 2 h but not detectable at 12 or 24 h after i.p. injection of SEB (Fig. 1A). In contrast, IL-17A was not detectable in SEB-injected wild-type C57BL/6 mice (Fig. 1A) and neither were several other cytokines tested (e.g., IFN-γ and IL-4). This highlights the requirement for human MHC class II molecules in the optimal activation of T cells by SAgs. The injection of SEB_{N23A}, a mutant version of SEB with impaired binding to Vβ8.2 TCR (29), into DR4tg mice also resulted in no detectable IL-17A in the serum (Fig. 1A), indicating that SEB-induced IL-17A production is highly T cell dependent.

We next tested a panel of bacterial SAgs other than SEB for their ability to induce IL-17A production in DR4tg mice. These included TSST-1, staphylococcal enterotoxin A (SEA), SpeA, streptococcal pyrogenic exotoxin I (SpeI), and streptococcal mitogenic exotoxin Z (SmeZ). TSST-1 administration did not result in IL-17A appearance in the serum and neither did SpeI or SmeZ (data not shown). As such, DR4tg mice do not appear to provide a suitable model in which to study the role of IL-17A in the context of TSST-1–mediated TSS or SpeI/SmeZ-triggered host responses. In

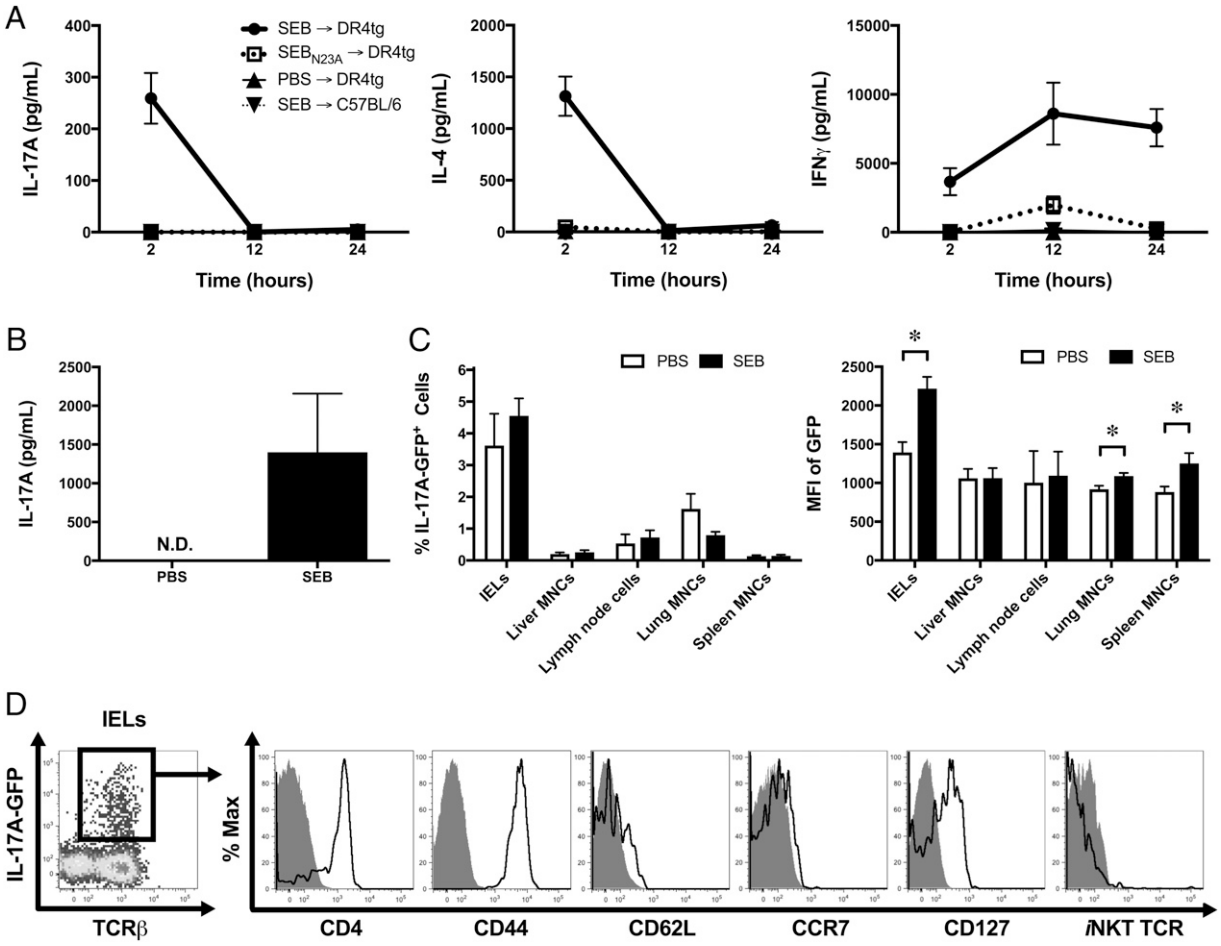

FIGURE 1. Rapid IL-17A production by $CD4^+$ T_{EM} cells in a humanized mouse model of TSS. (**A**) DR4tg mice were injected i.p. with 50 μg SEB, SEB_{N23A}, or PBS, and bled at indicated time points for serum cytokine measurements. Mean ± SEM values from two independent experiments are shown ($n = 4$). (**B**–**D**) IL-17A–GFP/DR4tg chimeric mice were injected i.p. with PBS or 50 μg SEB and sacrificed after 2 h. (B) Serum IL-17A levels in SEB- and PBS-treated IL-17A–GFP/DR4tg bone marrow chimeric mice were determined by ELISA. Mean values ± SEM from three independent experiments are shown ($n = 4$–5 mice per group). (C) The frequencies of IL-17A–GFP^+ cells and the geometric MFI of IL-17 were determined by flow cytometry among nonparenchymal mononuclear cells (MNCs) obtained from indicated organs of SEB- and PBS-treated mice. Mean values ± SEM from three independent experiments are shown ($n = 6$–7 per group). $*p \leq 0.05$, two-tailed Student t test. (D) The phenotype of IL-17A–GFP^+ cells among IELs from SEB-treated mice was determined using fluorochrome-conjugated Abs and tetramers for indicated markers (open black histograms) and isotype controls (filled, gray histograms). Representative dot plot and histograms from three independent experiments are shown ($n = 4$–6). N.D., not detectable.

contrast, animals injected with SEA and SpeA had detectable IL-17A levels in their serum (55 and 286 pg/ml, respectively). Therefore, the early IL-17A production may not be limited to staphylococcal TSS, and may also play a role in streptococcal infections. Of note, LPS, a potent stimulus that activates immune cells through a different mechanism than SAgs, failed to trigger an IL-17A response in DR4tg mice (data not shown).

To identify the cellular source of IL-17A, we generated IL-17A–GFP/DR4tg bone marrow chimeric mice. This system allows for quantification of IL-17A responses as measured by GFP fluorescence in SAg-sensitive, human MHC class II–expressing mice. Three weeks after the adoptive transfer of bone marrow cells, chimeric mice were injected with 50 μg SEB and sacrificed 2 h later to obtain blood, spleen, lymph nodes (cervical, axillary, brachial, mesenteric, inguinal, and popliteal), liver, lungs, and small intestine. When compared with PBS controls, which showed no detectable IL-17A in serum, SEB-injected chimeric mice produced substantial amounts of IL-17A after 2 h (Fig. 1B). The greatest frequency of IL-17A–expressing cells was found among IELs of the small intestine (Fig. 1C). Notably, the frequencies of IL-17A–expressing cells did not significantly differ between SEB and PBS treatment groups (Fig. 1C). However, the mean fluorescence intensity (MFI) of GFP, an indicator of IL-17A production on a per cell basis, increased upon in vivo SEB exposure in IELs and to a lesser degree among lung and splenic nonparenchymal mononuclear cells (Fig. 1C).

Having determined that IL-17A expression was highly upregulated and most abundant in the IEL compartment after SEB exposure, we next sought to immunophenotype these rapidly IL-17A–producing cells. The majority of $IL\text{-}17A^+$ cells were defined as $CD4^+$ T_{EM} cells due to their $TCR\beta^+CD4^+CD44^+CCR7^-CD62L^-CD127^+$ surface phenotype (Fig. 1D) (40). Similarly, $CD4^+$ T_{EM} cells constituted the majority of $IL\text{-}17A^+$ cells among IELs of PBS-treated mice (data not shown).

We previously reported that *i*NKT cells can be activated by group II bacterial SAgs, including SEB, leading to a swift cytokine response (29). In addition, a subset of *i*NKT cells is capable of producing IL-17A in response to glycolipid Ags (41). Therefore, it was important to rule in or rule out the participation of *i*NKT-17 cells in our model. We found that in vivo stimulation with SEB gives rise to IL-17A–expressing cells that do not possess the canonical TCR of *i*NKT cells as judged by their lack of

staining with α-galactosylceramide–loaded CD1d tetramer (Fig. 1D).

As a confirmatory approach, we generated D17 mice by crossing DR4tg mice with IL-17A–GFP reporter animals. We found a pattern similar to that observed in the bone marrow chimeras, namely increased IL-17A MFI among IELs of SEB-primed D17 mice (Supplemental Fig. 1). IL-17A–producing cells in D17 mice also similarly exhibited a T_{EM} phenotype. Having an adequate supply of D17 animals enabled us to additionally investigate the lamina propria, a site in which IL-17A–secreting T cells are known to be abundant (42). These experiments revealed that systemic exposure to SEB raises both the frequency of IL-17A$^+$CD4$^+$ T_{EM} cells in the lamina propria and the intensity of IL-17A production by these cells. In fact, the IL-17A response was stronger in the LPL compartment in comparison with IELs (Supplemental Fig. 1).

Together, the above findings show that select SAgs induce rapid IL-17A production by CD4$^+$ T_{EM} cells in a clinically relevant mouse model of TSS. The IL-17A response by mouse CD4$^+$ T_{EM} cells requires high-affinity interactions between SAgs and human MHC, and is most pronounced among intestinal IELs and LPLs.

SAgs induce a rapid IL-17A response by human PBMCs in vitro

After we established that SAgs were able to stimulate early IL-17A production in DR4tg mice, we assessed whether SAgs also elicit IL-17A responses in human PBMCs. First, PBMCs from healthy donors were stimulated with SEB or TSST-1 and analyzed for changes in cytokine mRNA levels by qPCR. Samples from all donors showed massive IL-17A mRNA upregulation after stimulation by SEB and, to a slightly lesser extent, by TSST-1 (Fig. 2A). IL-17A mRNA was highly upregulated at 2 h, reached a maximum at 4 h, and gradually decreased until 24 h poststimulation (Fig. 2A). Interestingly, the magnitude and the kinetics of the IL-17A mRNA response differed considerably when compared with IFN-γ (Fig. 2A, 2B), a prototypic proinflammatory cytokine that is induced by SAgs in humans (43) and that is considered pathogenic in mouse models of TSS (44). IL-17A mRNA upregulation was far greater in magnitude at early time points and began to decline after 4 h whereas IFN-γ mRNA levels steadily increased until 24 h (Fig. 2A, 2B).

To ascertain whether human IL-17A was actively secreted among other rapidly produced inflammatory mediators (43), culture supernatants from SAg-stimulated PBMCs were assayed for cytokines by bead-based multiplexing. Both SEB and TSST-1 provoked rapid IL-17A and IFN-γ responses, which were detectable as early as 2 h and continued to accumulate by 24 h (Fig. 2C). The inflammatory cytokines TNF-α and IL-6, as well as the growth-promoting cytokine IL-2, were also produced within hours of SAg stimulation (Fig. 2D). Although the kinetics of cytokine expression was consistent for both SEB and TSST-1 stimulation, SEB elicited a more robust response for most cytokines tested when compared with TSST-1 (Fig. 2C, 2D).

Thus far, our findings revealed an unexpected discordance vis-à-vis the kinetics of IL-17A expression at mRNA and protein levels; that is, whereas IL-17A mRNA was rapidly upregulated and gradually declined after 4 h, IL-17A protein continued to accumulate in the supernatant up to 24 h (Fig. 2A, 2C). This discordance was especially apparent when compared with the IFN-γ expression kinetics that followed a similar pattern for both cytokine mRNA and protein (Fig. 2B, 2C). We hypothesized that disparities in mRNA stability between IL-17A and IFN-γ may account for the noted differences as more stable mRNA may not require consistent upregulation for translation into increasing amounts of protein. Because the degree of IL-17A mRNA stability in primary human T cells was unknown, we tested our hypothesis by comparing the half-lives of IL-17A and IFN-γ mRNA in SEB-stimulated PBMC cultures using the transcriptional inhibitor act-D (45). PBMCs were challenged with SEB for 4 h consistent with the IL-17A mRNA response peak (Fig. 2A), treated with act-D, and analyzed for cytokine mRNA expression in the subsequent 8 h after transcriptional arrest. Intriguingly, whereas IFN-γ mRNA was quickly degraded within the first few hours, IL-17A mRNA expression remained remarkably stable after the addition of act-D (Fig. 2E).

These results indicate that SAgs potently activate human PBMCs to rapidly upregulate IL-17A mRNA and secrete IL-17A protein within hours. Interestingly, the initial IL-17A mRNA upregulation is greater in magnitude and yields more stable mRNA in comparison with the canonical inflammatory cytokine IFN-γ although both cytokines are quickly secreted in culture.

SAg-exposed human CD4$^+$ effector memory T cells are rapid and potent producers of IL-17A

As this work provides the initial report of IL-17A secretion in human PBMCs within the first few hours of SAg exposure, we next aimed to identify its cellular source. Exposure to either SEB or TSST-1 resulted in substantial intracellular IL-17A production by CD3$^+$ T cells within 4 h (Fig. 3A). SEB was significantly more potent than TSST-1 and caused IL-17A production by 0.182% of all PBMCs (Fig. 3A). The MFI of IL-17A staining was equivalent though, indicating that SEB- and TSST-1–stimulated cells synthesized similar amounts of IL-17A on a per cell basis (Fig. 3A). We also observed that IL-17A$^+$ cells among TSST-1–stimulated PBMCs showed reduced CD3 expression suggesting partial TCR downregulation. Lastly, we confirmed that only CD3$^+$ T cells were actively secreting IL-17A using a cytokine secretion assay in which IL-17A that is about to be secreted binds to the cell surface via a bivalent Ab molecule specific for both CD45 and IL-17A (data not shown).

To immunophenotype IL-17A–producing cells, PBMCs were challenged with SEB for 4 h and analyzed for a variety of surface markers and transcription factors by flow cytometry. The vast majority of IL-17A$^+$ cells expressed high levels of CD4 and CD45RO, and were CCR7$^-$ (Fig. 3B), indicating a surface phenotype characteristic of CD4$^+$ T_{EM} cells (46). In line with previous studies (47–49), IL-17A$^+$ cells also expressed CCR6 and the transcription factor RORγT (Fig. 3B), which are hallmarks of the Th17 lineage. Notably, the majority of IL-17A$^+$ cells expressed the lectin receptor CD161 (Fig. 3B). CD161 is highly expressed on innate-like T cells including γδ T, MAIT, and *i*NKT cells but only moderately expressed on Th17 cells (50). Thus, we investigated γδ TCR, Vα7.2 TCR and *i*NKT TCR expression to rule in/out γδ T, MAIT, and *i*NKT cells, respectively (Fig. 3B). These innate-like T cell subsets, in addition to a small population of CD8$^+$ T cells, constituted only minor fractions of the overall IL-17A$^+$ cell population (Fig. 3C). In contrast, CD4$^+$ T_{EM} cells were the dominant IL-17A–expressing population, which comprised >75% of IL-17A$^+$ cells (Fig. 3C).

Strikingly, our results revealed thus far that only a small fraction of PBMCs produced IL-17A protein in response to SAgs (Fig. 3A) despite the massive upregulation of IL-17A mRNA observed in bulk PBMCs (Fig. 2A). We initially postulated that other cell types in addition to CD4$^+$ T_{EM} cells contributed to the substantial IL-17A mRNA response, but were not detectable by intracellular IL-17A staining. To

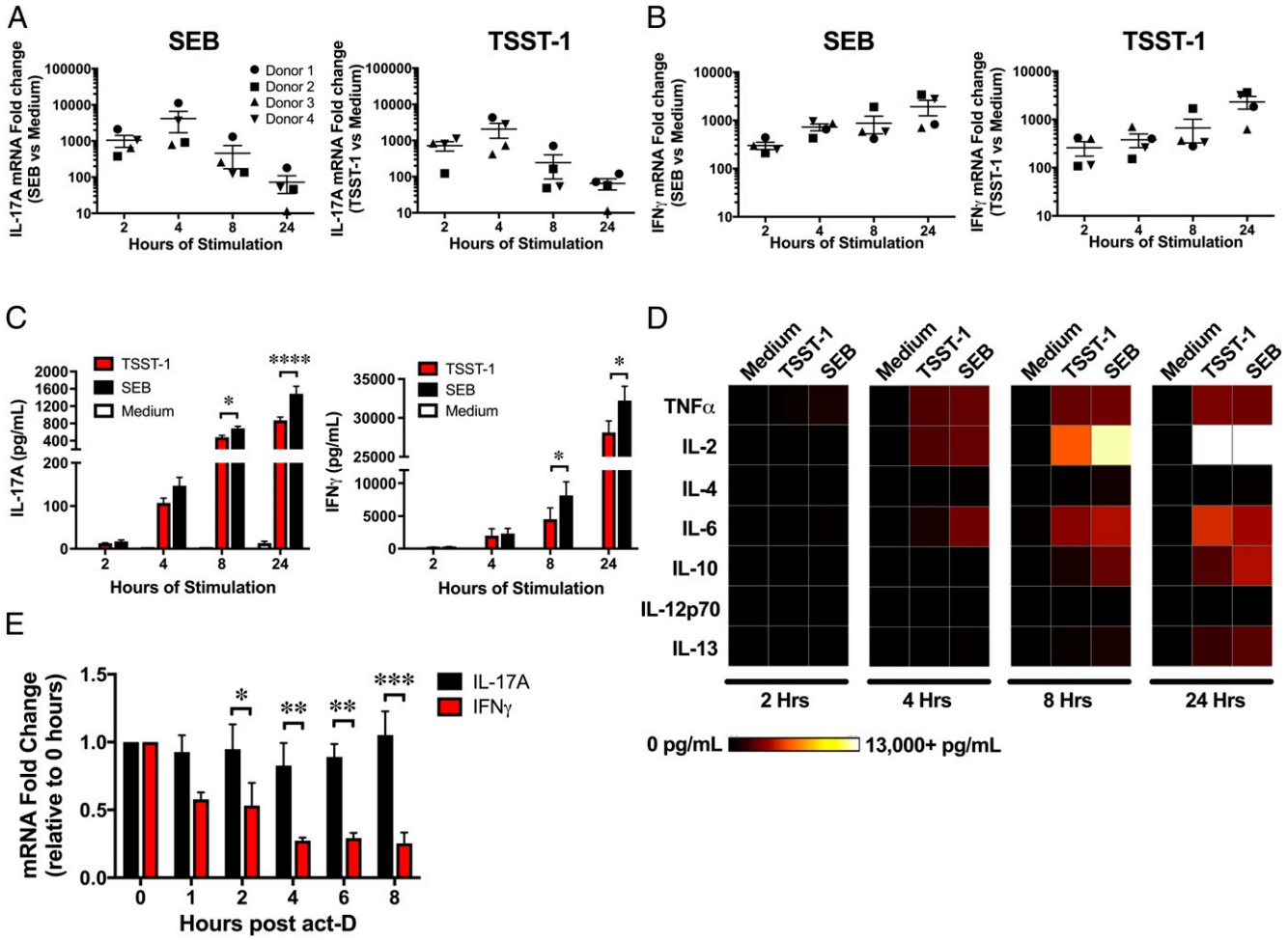

FIGURE 2. SAgs induce rapid IL-17A synthesis by human PBMCs. Human PBMCs were left untreated or stimulated with 100 ng/ml SEB or TSST-1 for indicated durations. (**A**) IL-17A or (**B**) IFN-γ mRNA upregulation in SAg-stimulated PBMCs was determined by qPCR. Data are shown as fold change relative to unstimulated medium control at each time point. (**C** and **D**) Cytokine concentrations in the supernatant of SAg-stimulated PBMCs at indicated time points were determined by bead-based cytokine multiplexing. Mean values ± SEM from four individual donors are shown. Statistical comparisons were made by two-way ANOVA ($p \leq 0.0001$) with Holm–Sidak post hoc analysis). (**E**) Human PBMCs were stimulated with SEB for 4 h prior to act-D treatment. IL-17A and IFN-γ mRNA fold changes normalized to time zero (i.e., addition of act-D) were determined by qPCR. Data pooled from three individual donors are shown. Statistical comparisons were made by two-way ANOVA ($p = 0.0072$) with Holm–Sidak post hoc analysis. *$p \leq 0.05$, **$p \leq 0.01$, ***$p \leq 0.001$, ****$p \leq 0.0001$.

address this, we used the PrimeFlow RNA assay, a new technology that utilizes fluorescent in situ hybridization to enable simultaneous detection of cells expressing IL-17A mRNA and intracellular IL-17A protein by flow cytometry. As expected, SEB stimulation enhanced the expression of IL-17A mRNA (Fig. 3D). Moreover, $CD4^+$ T_{EM} cells ($CD3^+CD45RO^+CCR7^-$) comprised the majority of IL-17A $mRNA^+$ cells (Fig. 3D), consistent with our intracellular IL-17A protein findings (Fig. 3C). Notably, a small proportion of IL-17A mRNA-producing $CD4^+$ T cells stained positively for CCR7 (Fig. 3D), indicating that $CD4^+$ central memory T cells may be a source of IL-17A protein at later time points. These results indicate that $CD4^+$ T_{EM} cells are primarily responsible for rapid IL-17A secretion among SAg-stimulated PBMCs despite their relative rarity.

As multicytokine-producing T cells are reportedly induced by SEB stimulation at relatively late time points (51), we explored whether early IL-17A producers would also coexpress IFN-γ. Surprisingly, only a minute subset of IL-17A/IFN-γ coexpressors was detectable following SAg stimulation over a 4 h period, and the overwhelming majority of cytokine-producing cells exclusively expressed either IL-17A or IFN-γ (Fig. 4A). A similar trend for IL-17A and IFN-γ expression was also evident at 24 h post–SAg stimulation (Fig. 4B). Interestingly, at 4 h post-SEB, $CD4^+$ T_{EM} cells constituted a large proportion of IFN-γ^+ cells (Fig. 4C), similar to IL-$17A^+$ cells observed above. This finding prompted us to examine whether IL-17A–producing $CD4^+$ T_{EM} cells had the potential to produce IFN-γ mRNA, but were not synthesizing appreciable amounts of IFN-γ protein. We found that only a small fraction of IL-$17A^+$ cells showed detectable IFN-γ mRNA transcripts (Fig. 4D).

Collectively, the above results indicate that SAg-based stimulation of human PBMCs induces a rapid and potent IL-17A response that is chiefly mediated by $CD4^+$ T_{EM} cells. Although $CD4^+$ T_{EM} cells are responsible for substantial early IFN-γ production as well, the IL-17A– and IFN-γ–producing subsets were two independent populations.

IL-17RA blockade reduces inflammatory gene expression in staphylococcal enterotoxin B–exposed human PBMCs and secondarily activated dermal fibroblasts

Many downstream targets of IL-17A signaling are inflammatory cytokines and chemokines (52), which likely augment or

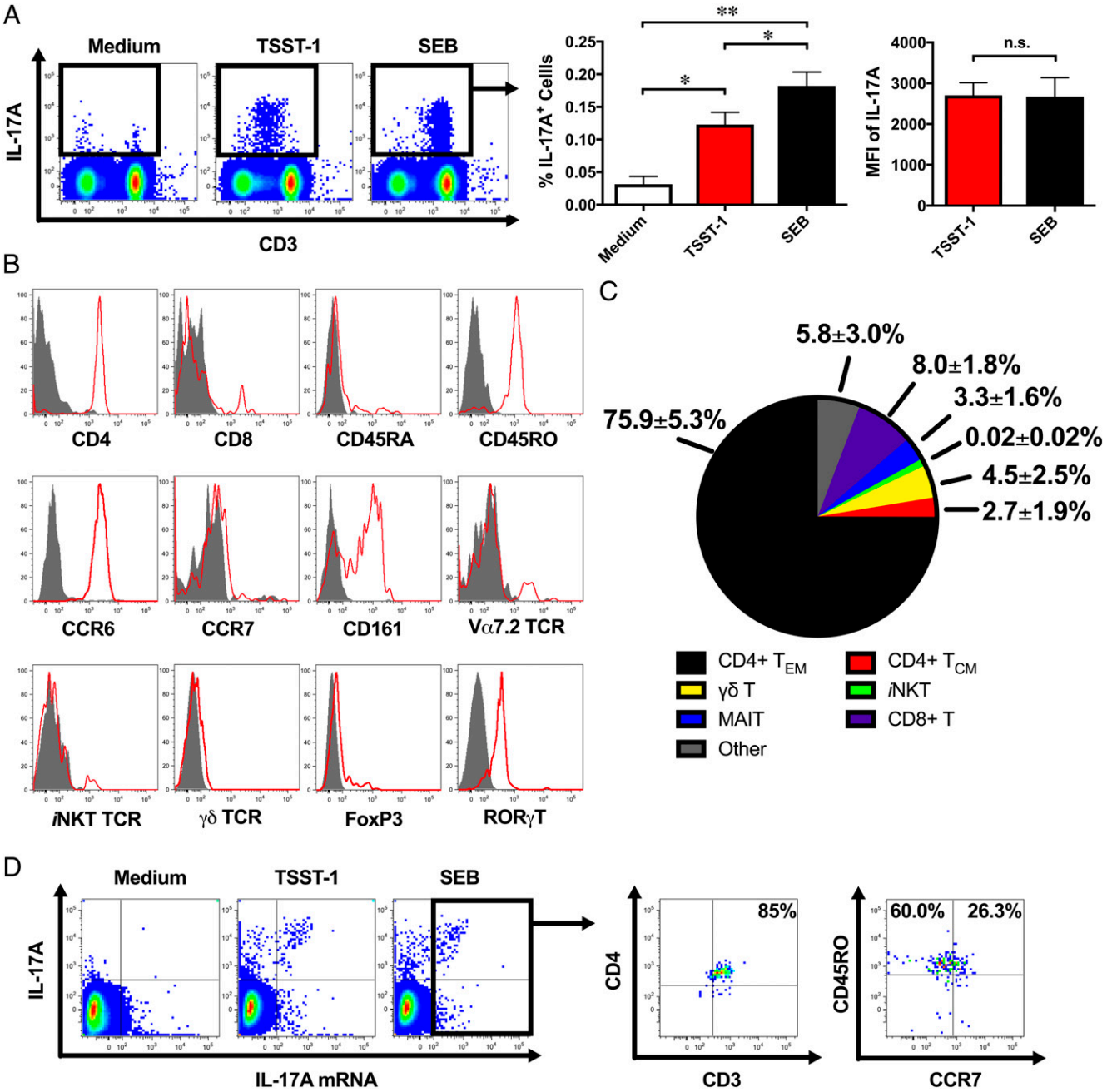

FIGURE 3. $CD4^+$ T_{EM} cells are the major source of IL-17A in SAg-stimulated human PBMCs. Human PBMCs were left untreated in medium or stimulated with 100 ng/ml SEB or TSST-1 for 4 h. (**A**) IL-17A–producing cells were identified by intracellular cytokine staining and further analyzed by flow cytometry. Representative dot plots of SAg-stimulated PBMCs are depicted. The percentage of IL-17A–expressing cells and geometric MFI of IL-17A are shown as mean values ± SEM for six individual donors. One-way ANOVA ($p = 0.0007$) with Holm–Sidak post hoc analysis was used (* $p \leq 0.05$, ** $p \leq 0.01$); n.s., not significant by two-tailed Student t test. (**B**) $IL\text{-}17A^+$ cells were immunophenotyped based on their expression of indicated cell surface and intracellular markers (open red histograms) relative to isotype control (filled, gray histograms). Illustrated data represent four individual donors displaying similar results. (**C**) Values represent mean percentages ± SEM of four individual donors. Subtypes were defined as: $CD4^+$ T_{EM} ($CD4^+CD3^+CD45RO^+CCR7^-$), $CD4^+$ T_{CM} ($CD4^+CD3^+CD45RO^+CCR7^+$), γδ T (γδ TCR^+), *i*NKT ($CD3^+CD1d$ tetramer$^+$), MAIT ($CD3^+$Vα7.2 TCR^+CD161^+), $CD8^+$ T ($CD3^+CD4^-CD8^+$). (**D**) IL-17A protein and mRNA coexpressing cells were identified using the PrimeFlow RNA technology and analyzed by flow cytometry. Dot plots are representative of four individual donors. T_{CM}, central memory T cells.

perpetuate the overwhelming inflammatory cascade encountered in TSS. Accordingly, stimulation of human PBMCs with SEB for 8 h resulted in upregulation of many different pro- and anti-inflammatory genes known to be modulated by IL-17A (Supplemental Table III). Also highly upregulated was the related inflammatory cytokine IL-17F, which signals through the same IL-17RA/IL-17RC complex (53). Thus, we sought to evaluate the contribution of IL-17RA signaling to induction of inflammatory genes in the initiation of the cytokine storm.

PBMCs were preincubated with a blocking IL-17RA mAb or isotype control, stimulated with SEB for 8 h, and evaluated for changes in gene expression by qPCR. IL-17RA blockade resulted in diminished expression of several key inflammatory cytokines involved in TSS, including TNF-α, IFN-γ, and IL-6 (Fig. 5A). Additionally, the expression of many chemokines such as CCL5,

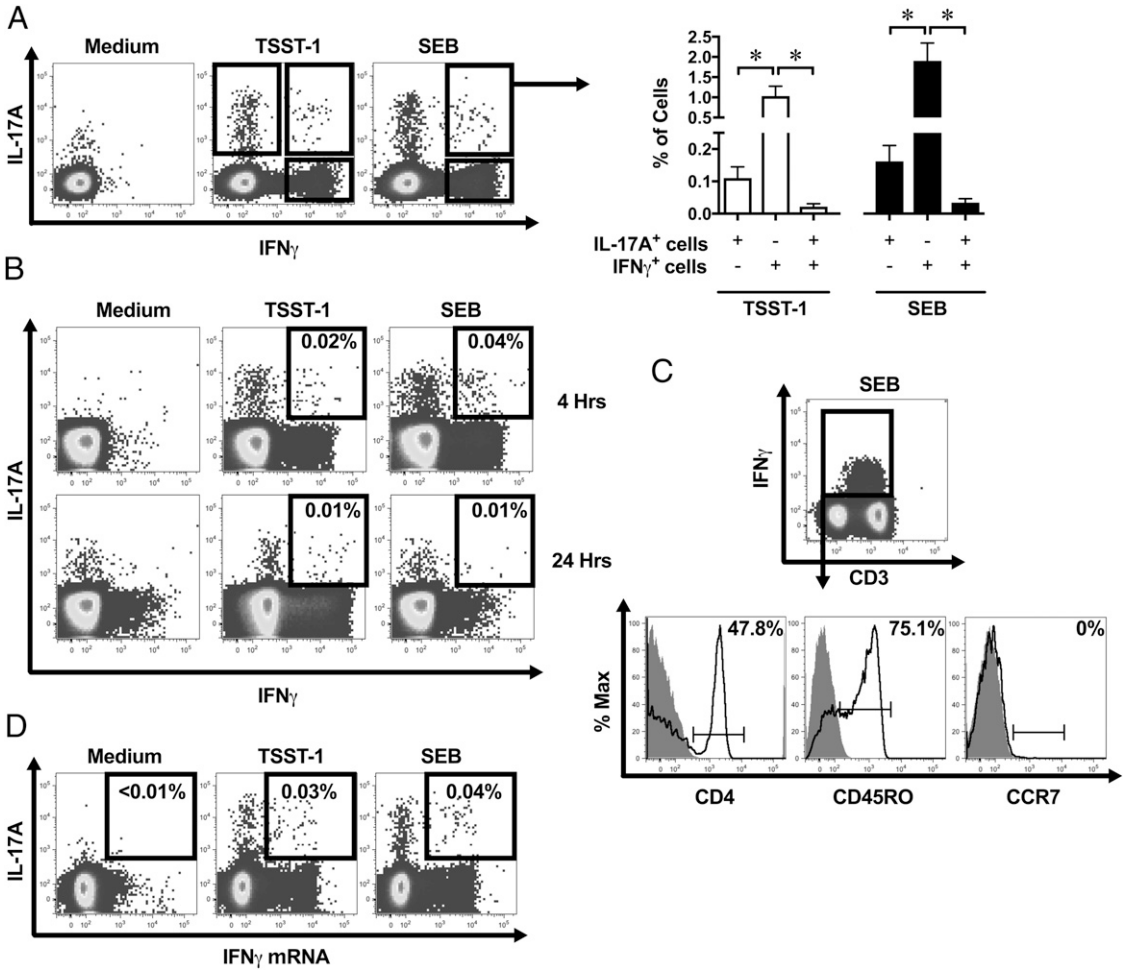

FIGURE 4. SAg-stimulated IL-17A– and IFN-γ–producing cells are two distinct populations. Human PBMCs from healthy volunteers were left untreated or stimulated with 100 ng/ml SEB or TSST-1 for 4 h (**A**, **C**, and **D**) or 4 h and 24 h (**B**). IL-17A– and IFN-γ–producing cells were identified by intracellular cytokine staining and quantified by flow cytometry. Representative dot plots of SAg-stimulated PBMCs and mean percentages ± SEM from two to four individual donors are shown. Statistical comparisons were made by one-way ANOVA ($p = 0.0255$ and $p = 0.0224$ for SEB and TSST-1 treatment conditions, respectively) with Holm–Sidak post hoc analysis (*$p \leq 0.05$). (C) Gated IFN-γ–producing cells were immunophenotyped by their expression of surface markers (open black histograms) relative to isotype control (filled, gray histograms). Data are representative of four individual donors. (D) IL-17A and IFN-γ mRNA coexpressing cells were identified using the PrimeFlow RNA technology and analyzed by flow cytometry. Dot plots are representative of four individual donors.

CCL7, CXCL1, and CXCL6 were highly downregulated. Interestingly, the blockade of IL-17RA signaling also resulted in upregulation of notable anti-inflammatory cytokines IL-4, TGF-β1, and IL-10 (Fig. 5A). It is noteworthy that in these experiments, we chose to work with a mAb dose (i.e., 10 μg/ml) that was previously reported to efficiently block IL-17RA (54, 55). In a limited number of experiments, we reconfirmed that this dose could significantly inhibit the upregulation of CEBPD, a transcription factor linked to acute inflammatory conditions (56), in SEB-exposed PBMCs. In contrast, a 0.1 μg/ml dose of anti–IL-17RA was completely ineffective, and a 1 μg/ml dose inhibited CEBPD upregulation only marginally (data not shown).

In the next series of experiments, we used a human PBMC-dermal fibroblast coculture system to mimic the secondary effect of IL-17A signaling in nonhematopoietic cells. To this end, PBMCs and fibroblasts were cultured in physically separate compartments prior to SEB stimulation. We found an ∼3-fold increase in the expression level of CEBPD by dermal fibroblasts that were cocultured with SEB-primed PBMCs (Fig. 5B). Importantly, this response was abrogated in the presence of 10 μg/ml anti–IL-17RA mAb. Also as expected, SEB did not change the expression of CEBPD in fibroblasts alone, a condition that was used as a control (Fig. 5B).

Taken together, the above findings strongly suggest that IL-17RA signaling plays an important proinflammatory role in TSS by increasing the expression of inflammatory mediators that are expected to contribute to TSS pathogenesis.

IL-17A is pathogenic in an in vivo model of toxic shock syndrome

Because the cytokine storm drives many symptoms of TSS, attenuation of rapidly produced cytokines that further perpetuate the inflammatory cascade, such as IL-17A, may be of prime importance to reduce TSS severity. Furthermore, IL-17A functions through induction of inflammatory mediators in both hematopoietic and nonhematopoietic compartments (19). Thus, we used the DR4tg mouse model, which provides a powerful in vivo system in which to delineate the role of early IL-17A responses in TSS. We treated DR4tg mice with an anti–IL-17A mAb 3 h prior to and 1 h after the administration of SEB and monitored disease progression. Neutralizing IL-17A at the TSS onset

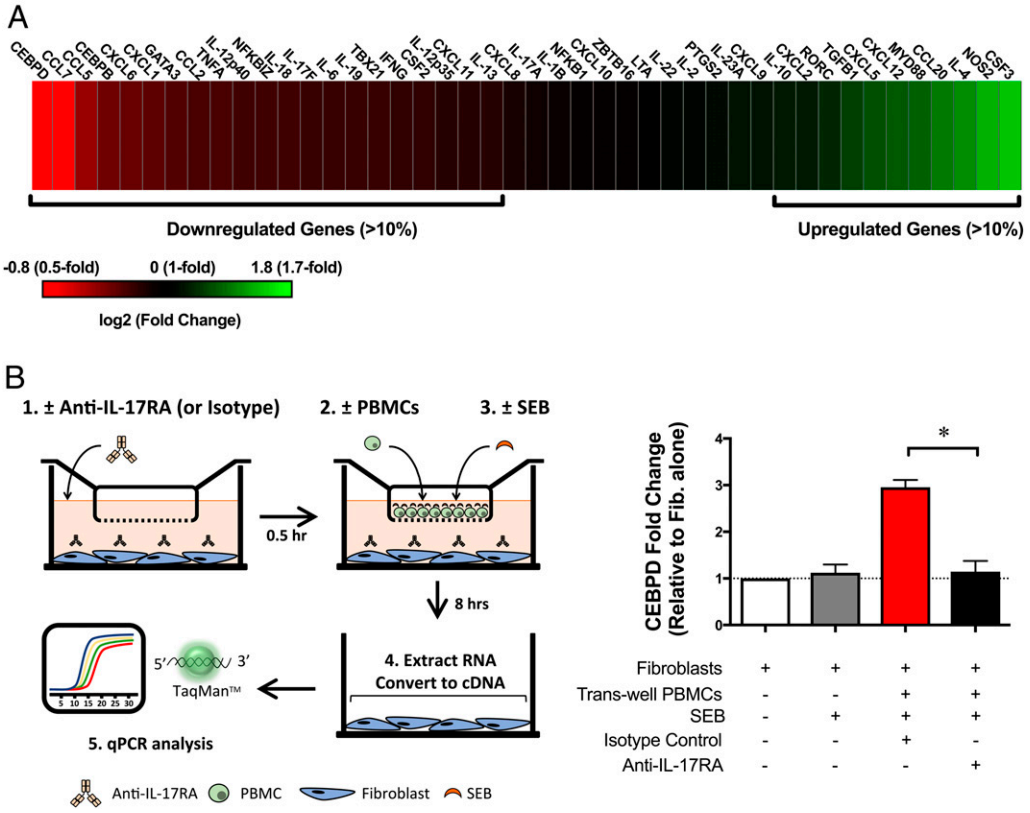

FIGURE 5. Blockade of IL-17RA signaling attenuates SEB-induced inflammatory gene expression in human PBMCs and in downstream nonhematopoietic cells. (**A**) Human PBMCs were preincubated with 10 μg/ml anti–IL-17RA blocking Ab or isotype control and subsequently stimulated with 100 ng/ml SEB for 8 h. Changes in gene expression were determined by qPCR and represented as log2 (fold change) of the anti–IL-17RA group normalized to isotype control. Differentially regulated genes were defined as a >10% fold change difference between treatment groups. Fold changes in gene expression were pooled from three individual donors and are represented as mean values. (**B**) Human dermal fibroblasts were grown in a flat-bottom plate and cocultured with human PBMCs that were seeded into a cell culture insert with a permeable membrane. Fibroblasts and PBMCs were in two physically separate compartments. Cocultures were left untreated or stimulated with 100 ng/ml SEB. Eight hours later, the insert was removed and fibroblasts were harvested and examined by qPCR for their CEBPD expression. Anti–IL-17RA or isotype control (10 μg/ml each) was added 30 min before SEB stimulation as indicated. Fold changes in CEBPD gene expression relative to the fibroblast-only condition was calculated for three PBMC samples prepared from three individual donors. Data are shown as mean ± SEM (* $p \leq 0.05$, two-tailed Student t test).

resulted in significantly attenuated weight loss as early as 20 h after SEB injection (Fig. 6A). Importantly, by 7 d after SEB injection, 67% of mice that were treated with anti–IL-17A, compared with only 27% of mice receiving the isotype control, had survived (Fig. 6B).

Because TSS is characterized by multiorgan dysfunction, we investigated whether IL-17A neutralization affects SAg-induced liver and intestinal damage. DR4tg mice receiving SEB and either an anti–IL-17A mAb or an isotype control were sacrificed at 48 h post-SEB, and liver and the small intestine were collected for histopathological analyses. SEB induced moderate periportal inflammation in the livers of both anti–IL-17A– and isotype control–treated mice (Fig. 6C). However, hepatic steatosis, an early indication of hepatotoxicity (57), was greatly reduced in anti–IL-17A–treated mice compared with those receiving the isotype control (Fig. 6C). Furthermore, the small intestines of mice receiving anti–IL-17A showed less inflammation, epithelial cell damage, and villar blunting compared with the control cohort (Fig. 6C). As scored by a veterinary pathologist blinded to the cohorts, the overall TSS pathology for mice receiving anti–IL-17A was significantly reduced (Fig. 6D). Finally, we found a statistically significant decrease in the serum concentration of IL-6, a downstream target of IL-17A signaling, in anti–IL-17A–treated mice 2 h after SEB administration (Fig. 6E).

Collectively, to our knowledge, these results provide the first report that IL-17A is pathogenic in TSS and that neutralizing IL-17A ameliorates morbidity, mortality, and tissue damage in a humanized mouse model of TSS.

Discussion

The inflammatory response mediated by IL-17A is the result of the induction and activation of a large network of immune effector molecules including cytokines, chemokines, acute phase reactants, tissue remodeling enzymes, antimicrobial peptides, and transcription factors (19). In this way, IL-17A plays a critical role in the immune response against many different pathogens including *S. aureus* (58) and *S. pyogenes* (59). However, unbalanced or dysregulated IL-17A responses may also lead to excessive inflammation and can therefore be detrimental in several diseased states (52). In this study, we report a pathogenic role for IL-17A during infection.

Much of the existing knowledge of TSS pathogenesis has relied on conventional mouse models (12). However, SAgs exhibit poor affinity for certain mouse MHC class II molecules (34), and as a result, many strains of laboratory mice are resistant to TSS. Sensitizing agents such as D-galactosamine (60) or LPS (61) have been employed to amplify the effects of SAgs and induce lethality, but the extent to which these models accurately reflect human TSS is questionable. For example, D-galactosamine pretreatment leads

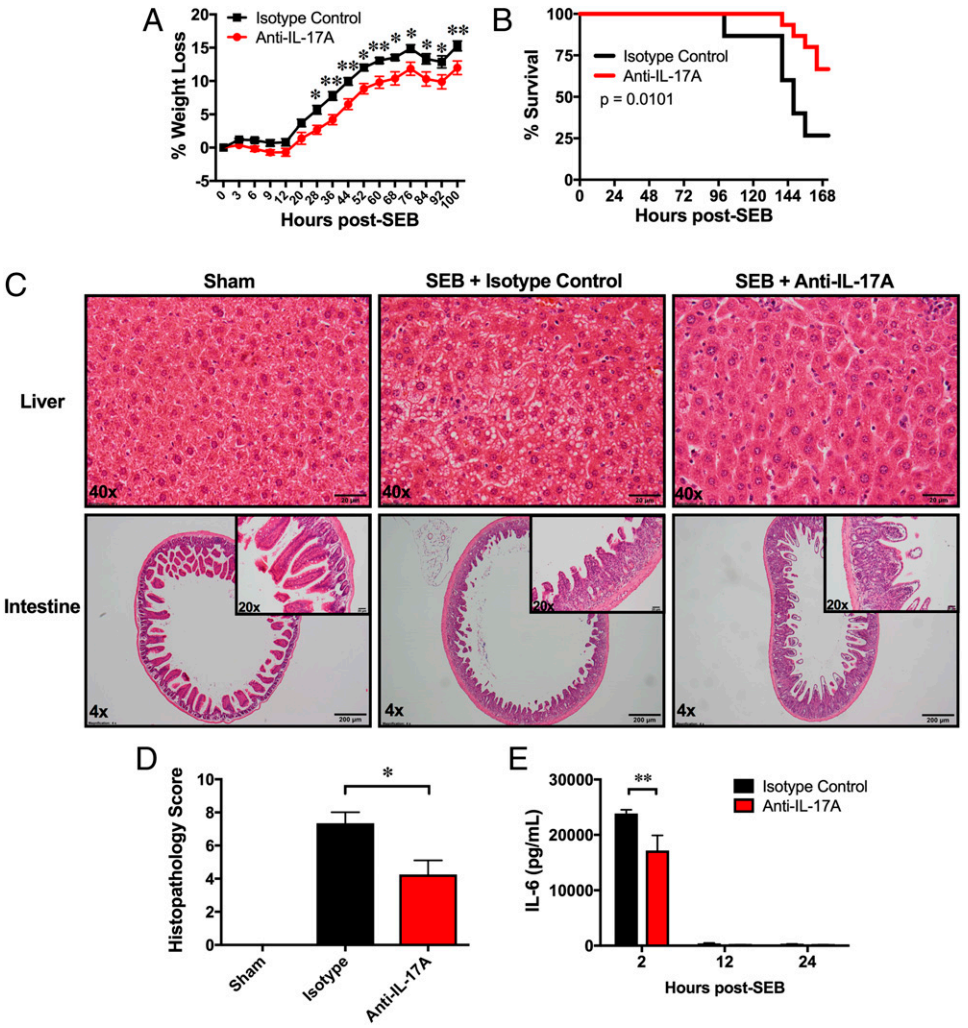

FIGURE 6. IL-17A neutralization in a humanized mouse model of TSS reduces morbidity, mortality, and tissue damage. DR4tg mice were injected i.p. with 200 μg anti–IL-17A neutralizing Ab or isotype control 3 h before and 1 h after receiving 100 μg SEB. (**A**) Weight loss was monitored every 3 h for the first 12 h and every 8 h thereafter (n = 15 per group). Two-way ANOVA was used (p = 0.0012) with Holm–Sidak post hoc analysis. *$p \leq 0.05$, **$p \leq 0.01$. (**B**) Survival was monitored up to 7 d after SEB (n = 15 per group). Mice were sacrificed when moribund (≥20% weight loss). $p = 0.0101$, log-rank test. (**C** and **D**) At 48 h after SEB injection, mice were sacrificed for their organs and H&E staining was performed as per standard protocols. Sections were scored by a veterinary pathologist blinded to the experimental conditions. Histopathology scores represent sum of changes in the liver (periportal inflammation + microvesicular steatosis) and small intestine (inflammatory cell infiltration + mucosal score [epithelial cell damage + villar blunting]) observed in each section. Parameters received scores from 0 to 3, with 0 = normal, 1 = mild, 2 = moderate, and 3 = severe, and were analysed using two-tailed Student t test. Stained sections are representative of sham (n = 2), SEB + isotype control (n = 3) and SEB + anti–IL-17A (n = 4) groups. Mean ± SEM values are shown. (**E**) Two hours after SEB injection, anti–IL-17A– and isotype control–treated mice (n = 4 per group) were bled and the IL-6 content of serum samples was quantified by ELISA. Mean ± SEM values are shown. Two-way ANOVA was used (p = 0.05) with Holm–Sidak post hoc analysis. *$p \leq 0.05$, **$p \leq 0.01$.

to extreme sensitivity to TNF-α–induced apoptosis in hepatocytes (62), which causes rapid mortality solely due to fulminant hepatitis, which does not represent human TSS (63). Here, we investigated SAg-induced cytokine responses utilizing DR4tg mice that transgenically express the human MHC class II molecule HLA-DR4. This allows for high-affinity SAg–MHC class II interactions resulting in robust activation of T cells and a cytokine storm that, if left untreated, simulates the potentially catastrophic human TSS (35–37).

We found that exposure of DR4tg mice to SEB resulted in swift production of several cytokines in serum, including the inflammatory cytokine IL-17A. Cytokines secreted in the early phase of the cytokine storm are especially important as they trigger endothelial cell damage that compromises vascular homeostasis and precipitates multiorgan dysfunction (64). Furthermore, rapid secretion of IL-17A not only has inflammatory effects on a wide variety of cell types throughout the body, it can directly induce and also synergize with other cytokines that are produced in the same timeframe. Other studies have found mouse IL-17A secretion in response to SAgs (36, 44, 65). IL-17 is also reportedly detectable in SEB-stimulated human PBMC cultures, albeit at relatively late time points (66, 67). Here, we demonstrate that very early IL-17A is of $CD4^+$ T_{EM} cell origin in mice and in human PBMC cultures. Furthermore, we show that the rapid induction of IL-17A, in addition to other cytokines, is dependent on T cell stimulation because the injection of DR4tg mice with a TCR-binding mutant form of SEB (SEB_{N23A}) resulted in minimal cytokine secretion. We believe the observed presence of IFN-γ, at moderate levels, after SEB_{N23A} exposure is likely the consequence of SEB engaging T cells that bear Vβ domains other than Vβ8.2 (29). Lastly, we extended our investigation to other SAgs and found that SpeA and SEA could also induce early IL-17A secretion.

Therefore, we propose that rapid IL-17A secretion plays a pathogenic role in both staphylococcal and streptococcal TSS.

To identify the location of IL-17A production in DR4tg mice, we generated IL-17A–GFP/DR4tg bone marrow chimeric mice as well as D17 mice in which IL-17A expression can be quantified by GFP fluorescence. Using these models, we found an increase in the frequency of IL-17A$^+$ cells and/or the signal intensity of IL-17A in several tissues, but chiefly among IELs and LPLs from the small intestine, upon exposure to SEB. Interestingly, although IL-17A was consistently absent from the serum of PBS-injected mice, IL-17A–producing cells were readily detectable in these animals, suggesting that IL-17A is expressed at basal levels in multiple organs. This observation is in agreement with those of previous investigations utilizing alternatively generated IL-17A–GFP mice (68) or IL-17A fate-mapping reporter mice (69) that showed resting levels of IL-17A among cells of the small intestine. We expand on these findings to implicate CD4$^+$ T_{EM} cells as the main source of constitutively expressed IL-17A in naive mice. Nevertheless, it stands to reason that additional sources/locations of IL-17A may also exist.

Memory T cells are highly enriched in the intestinal mucosa and their propensity for immediate effector function upon reactivation (70) puts them in a unique position to be rapidly activated by SAgs. It has also been suggested that SAgs produced in the intestinal tract by food-borne pathogens may cross the gut mucosa directly (71), placing memory T cells among the first responders to SAgs. In support of this hypothesis, IL-17A was preferentially induced in the intestinal epithelial layer by CD4$^+$ T_{EM} cells when mice were exposed to SEB. Furthermore, a study by Tilahun et al. (36) demonstrated that most NF-κB expression in SEB-injected HLA-DR3 mice was induced in the intestines.

The IL-17A response to SEB in mice appears to be translatable to humans, as PBMCs from healthy human volunteers stimulated with SAgs in vitro also exhibited rapid IL-17A production. IL-17A was secreted within hours of SAg exposure along with other inflammatory cytokines such as IFN-γ, TNF-α, and IL-6. This inflammatory profile was most pronounced within the first few hours of SAg stimulation, with anti-inflammatory cytokines IL-10 and IL-13 only reaching appreciable levels toward later time points. This pattern of expression provides additional evidence suggesting that potential therapies aimed at curbing the overwhelming cytokine storm in TSS may be most effective early after exposure to SAgs. A study by Krakauer et al. (72) supports this line of reasoning, where mice surviving TSS showed reduced inflammatory cytokine and chemokine levels, though not including IL-17A, at 8 h post-SEB administration. Furthermore, in a TSS model utilizing HLA-DR1 mice, lethality was prevented by anti–TNF-α treatment, which dampened the early but not the later phase of cytokine release (73). Therefore, it is likely that the early phase of the cytokine storm is responsible for TSS lethality and that attenuating this response may be a fruitful strategy to prevent mortality.

Unexpectedly, we observed apparently paradoxical differences between the kinetics of mRNA upregulation and resulting protein expression between IL-17A and IFN-γ responses in SAg-stimulated PBMCs. We propose that the variation of kinetics between the two cytokines may be due, at least in part, to differences in mRNA stability. However, the mechanisms of posttranscriptional regulation of IL-17A remain ill-defined. In mice, the RNA-binding protein Hu Ag R positively regulates IL-17A expression and mRNA stability (74). Conversely, another RNA-binding protein, tristetraprolin, binds directly to the 3′ untranslated region of IL-17A mRNA to mediate its decay (75). Lastly, the positive correlation between microRNAs and IL-17A expression in many diseases other than TSS also suggests that microRNAs may play a critical role in regulating IL-17A responses (76). Whether RNA-binding proteins or microRNAs posttranscriptionally regulate human IL-17A in TSS remains to be elucidated.

Our findings indicate that CD4$^+$ T_{EM} cells predominate in the early production of both IL-17A and IFN-γ in SAg-stimulated human PBMCs. We also observed that IL-17A and IFN-γ responses by CD4$^+$ T_{EM} cells were mutually exclusive, with only a small number of cells capable of producing both cytokines simultaneously. Thus, we propose that SAgs stimulate pre-existing and independent lineage-committed CD4$^+$ T_{EM} cell subsets to rapidly produce IL-17A (T_{EM}-17 cells) and IFN-γ (T_{EM}-γ cells) in the initial phases of the cytokine storm. Our results may extend the traditional paradigm of Th1-, Th2-, and Th17-lineages of activated effector CD4$^+$ T cells, which proceed to generate the body's long-lived pool of T_{EM} cells (77). This notion is supported by recent reports that human Th17 cells are a terminally differentiated T_{EM} cell population with a high capacity of self-renewal (78, 79).

The timing and the intensity of SAg stimulation in human PBMCs also apparently affect the phenotype and cytokine profiles of activated cells. We found that at 4 h post-SEB stimulation, IL-17A–producing CD4$^+$ T_{EM} cells exclusively expressed the Th17-lineage transcription factor RORγT but did not coproduce IFN-γ. In contrast, a recent study by Björkander et al. (80) demonstrated that 24-h stimulation of human PBMCs with SAgs induces IL-17A in CD4$^+$ T cells that express the regulatory T cell transcription factor FOXP3. As FOXP3 has been previously shown to be upregulated in SAg-stimulated CD4$^+$ T cells over days of SAg exposure (81), it remains to be seen whether early IL-17A–producing CD4$^+$ T_{EM} cells may acquire FOXP3 expression after longer periods of SAg stimulation. In a separate study, overnight stimulation of human PBMCs with 10 μg/ml SEB (a 100-fold greater concentration of SAg than the dose used in this study) induced multifunctional CD4$^+$ T_{EM} cells that often coexpressed IL-17A and IFN-γ (51). Both at 4 and 24 h after SAg stimulation, we detected only a minute subpopulation of coproducing CD4$^+$ T_{EM} cells. It is possible that the high concentration of SAg used by McArthur et al. (51) may have been responsible for the coproducer phenotype. Circulating levels of SAg in patients' serum samples range from ~40 pg/ml in intensive care units (82) to 50–100 ng/ml in adult burn patients (83), and as high as 1000 ng/ml in streptococcal TSS patients (84). As such, our findings utilizing a more conservative concentration of SAg may represent a more physiologically relevant outcome for SAg stimulation of human PBMCs.

We found that the blockade of IL-17RA signaling in SEB-stimulated PBMCs attenuated the expression of multiple inflammatory genes including IL-6, TNF-α, and IFN-γ, which mediate many toxic effects of TSS (12). Concomitantly, the expression of anti-inflammatory cytokine genes (IL-10, TGF-β1, and IL-4) was upregulated by IL-17RA blockade. To our surprise, CCL20, a chemokine that binds CCR6 to mobilize lymphocytes and dendritic cells, was also upregulated. Nevertheless, the overall picture emerging from our IL-17RA blockade experiments strongly suggests a proinflammatory role for IL-17RA signaling in the context of human PBMC responses to SAgs. Equally important, IL-17RA blockade in dermal fibroblasts prevented their secondary response to SEB-exposed PBMCs. Therefore, this approach may work at multiple levels and may have therapeutic potentials for TSS. When patients with severe plaque psoriasis were treated with brodalumab, a mAb against IL-17RA, reduced expression of inflammatory cytokine transcripts was noted (85). Our results are also supported by the findings of Crowe et al. (86) that IL-17RA knockout mice show greatly attenuated cytokine

storm when infected with influenza virus. In this model, the absence of IL-17RA signaling decreased lung inflammation, weight loss, and morbidity.

Remarkably, in vivo neutralization of IL-17A in DR4tg mice at the onset of TSS led to a significant reduction in weight loss and a striking increase in survival. We also observed drastic pathological changes in both the liver and the epithelium of the small intestine in DR4tg mice exposed to SEB. These mice developed hepatic microvesicular steatosis, an early toxic change in hepatocytes that signals serious disease. Characterized by the accumulation of small lipid vesicles in hepatocytes, microvesicular steatosis is indicative of impaired mitochondrial β-oxidation of fatty acids and can lead to multiorgan dysfunction (57). Importantly, microvesicular steatosis occurs in both human TSS (87, 88) and sepsis (89). To our knowledge, our work is the first description of its reversal in an animal model of TSS. We also observed considerable epithelial damage and villar blunting in the small intestine of mice injected with SEB. These pathological changes likely impair intestinal function and contribute to the weight loss observed in SAg-exposed mice. Importantly, in vivo neutralization of IL-17A in this model markedly attenuated both hepatic steatosis and damage to the intestinal epithelium. As almost all human TSS patients show multiorgan dysfunction (90), our results suggest that IL-17A may be an attractive clinical target to reduce TSS severity.

The key to successful treatment of TSS remains the rapid identification of the source of infection, appropriate and effective use of antibiotics, drainage of wounds (or removal of tampon in menstrual TSS), and supportive care (91). IVIg has also been shown to improve clinical outcomes in TSS caused by group A *Streptococcus* (92). However, there is currently no cure for the cytokine storm induced by SAgs. Here, we define the rapid production of IL-17A by $CD4^+$ T_{EM} cells as a novel mechanism underlying TSS immunopathology. Our findings suggest that neutralizing IL-17A function may serve to lessen systemic inflammatory cytokine levels and decrease tissue damage in TSS. Thus, a therapeutic approach targeting the early induction of multiple inflammatory mediators that are involved in the cytokine storm, including IL-17A, may be effective in averting TSS mortality.

Acknowledgments

We thank Dr. John Koval (Department of Epidemiology and Biostatistics, Western University) for expert statistical advice. We thank members of the Haeryfar laboratory for helpful discussions and Madeline Harvey for assistance with mouse irradiation.

Disclosures

The authors have no financial conflicts of interest.

References

1. McCormick, J. K., J. M. Yarwood, and P. M. Schlievert. 2001. Toxic shock syndrome and bacterial SAgs: an update. *Annu. Rev. Microbiol.* 55: 77–104.
2. Chesney, P. J., J. P. Davis, W. K. Purdy, P. J. Wand, and R. W. Chesney. 1981. Clinical manifestations of toxic shock syndrome. *JAMA* 246: 741–748.
3. Reingold, A. L., B. B. Dan, K. N. Shands, and C. V. Broome. 1982. Toxic-shock syndrome not associated with menstruation. A review of 54 cases. *Lancet* 1: 1–4.
4. Shands, K. N., G. P. Schmid, B. B. Dan, D. Blum, R. J. Guidotti, N. T. Hargrett, R. L. Anderson, D. L. Hill, C. V. Broome, J. D. Band, and D. W. Fraser. 1980. Toxic-shock syndrome in menstruating women: association with tampon use and *Staphylococcus aureus* and clinical features in 52 cases. *N. Engl. J. Med.* 303: 1436–1442.
5. Schlievert, P. M., K. N. Shands, B. B. Dan, G. P. Schmid, and R. D. Nishimura. 1981. Identification and characterization of an exotoxin from *Staphylococcus aureus* associated with toxic-shock syndrome. *J. Infect. Dis.* 143: 509–516.
6. Dinges, M. M., P. M. Orwin, and P. M. Schlievert. 2000. Exotoxins of *Staphylococcus aureus. Clin. Microbiol. Rev.* 13: 16–34.
7. Musser, J. M., A. R. Hauser, M. H. Kim, P. M. Schlievert, K. Nelson, and R. K. Selander. 1991. *Streptococcus pyogenes* causing toxic-shock-like syndrome and other invasive diseases: clonal diversity and pyrogenic exotoxin expression. *Proc. Natl. Acad. Sci. USA* 88: 2668–2672.
8. Dellabona, P., J. Peccoud, J. Kappler, P. Marrack, C. Benoist, and D. Mathis. 1990. Superantigens interact with MHC class II molecules outside of the antigen groove. *Cell* 62: 1115–1121.
9. White, J., A. Herman, A. M. Pullen, R. Kubo, J. W. Kappler, and P. Marrack. 1989. The V beta-specific SAg staphylococcal enterotoxin B: stimulation of mature T cells and clonal deletion in neonatal mice. *Cell* 56: 27–35.
10. Spaulding, A. R., W. Salgado-Pabón, P. L. Kohler, A. R. Horswill, D. Y. Leung, and P. M. Schlievert. 2013. Staphylococcal and streptococcal SAg exotoxins. *Clin. Microbiol. Rev.* 26: 422–447.
11. Krakauer, T., and B. G. Stiles. 2013. The staphylococcal enterotoxin (SE) family: SEB and siblings. *Virulence* 4: 759–773.
12. Krakauer, T., K. Pradhan, and B. G. Stiles. 2016. Staphylococcal SAgs spark host-mediated danger signals. *Front. Immunol.* 7: 23.
13. Dubinett, S. M., M. Huang, A. Lichtenstein, W. H. McBride, J. Wang, G. Markovitz, D. Kelley, W. W. Grody, L. E. Mintz, and S. Dhanani. 1994. Tumor necrosis factor-alpha plays a central role in interleukin-2-induced pulmonary vascular leak and lymphocyte accumulation. *Cell. Immunol.* 157: 170–180.
14. Mattsson, E., H. Herwald, and A. Egesten. 2003. Superantigens from *Staphylococcus aureus* induce procoagulant activity and monocyte tissue factor expression in whole blood and mononuclear cells via IL-1 beta. *J. Thromb. Haemost.* 1: 2569–2576.
15. Scheller, J., A. Chalaris, D. Schmidt-Arras, and S. Rose-John. 2011. The pro- and anti-inflammatory properties of the cytokine interleukin-6. *Biochim. Biophys. Acta* 1813: 878–888.
16. McKay, D. M., and P. K. Singh. 1997. Superantigen activation of immune cells evokes epithelial (T84) transport and barrier abnormalities via IFN-gamma and TNF alpha: inhibition of increased permeability, but not diminished secretory responses by TGF-beta2. *J. Immunol.* 159: 2382–2390.
17. Krakauer, T. 1999. Induction of CC chemokines in human peripheral blood mononuclear cells by staphylococcal exotoxins and its prevention by pentoxifylline. *J. Leukoc. Biol.* 66: 158–164.
18. Tessier, P. A., P. H. Naccache, K. R. Diener, R. P. Gladue, K. S. Neote, I. Clark-Lewis, and S. R. McColl. 1998. Induction of acute inflammation in vivo by staphylococcal SAgs. II. Critical role for chemokines, ICAM-1, and TNF-alpha. *J. Immunol.* 161: 1204–1211.
19. Korn, T., E. Bettelli, M. Oukka, and V. K. Kuchroo. 2009. IL-17 and Th17 Cells. *Annu. Rev. Immunol.* 27: 485–517.
20. Shen, F., and S. L. Gaffen. 2008. Structure-function relationships in the IL-17 receptor: implications for signal transduction and therapy. *Cytokine* 41: 92–104.
21. Cua, D. J., and C. M. Tato. 2010. Innate IL-17-producing cells: the sentinels of the immune system. *Nat. Rev. Immunol.* 10: 479–489.
22. Dusseaux, M., E. Martin, N. Serriari, I. Péguillet, V. Premel, D. Louis, M. Milder, L. Le Bourhis, C. Soudais, E. Treiner, and O. Lantz. 2011. Human MAIT cells are xenobiotic-resistant, tissue-targeted, CD161hi IL-17-secreting T cells. *Blood* 117: 1250–1259.
23. Murray, R. J. 2005. Recognition and management of *Staphylococcus aureus* toxin-mediated disease. *Intern. Med. J.* 35(Suppl. 2): S106–S119.
24. Kain, K. C., M. Schulzer, and A. W. Chow. 1993. Clinical spectrum of non-menstrual toxic shock syndrome (TSS): comparison with menstrual TSS by multivariate discriminant analyses. *Clin. Infect. Dis.* 16: 100–106.
25. Hajjeh, R. A., A. Reingold, A. Weil, K. Shutt, A. Schuchat, and B. A. Perkins. 1999. Toxic shock syndrome in the United States: surveillance update, 1979 1996. *Emerg. Infect. Dis.* 5: 807–810.
26. Descloux, E., T. Perpoint, T. Ferry, G. Lina, M. Bes, F. Vandenesch, I. Mohammedi, and J. Etienne. 2008. One in five mortality in non-menstrual toxic shock syndrome versus no mortality in menstrual cases in a balanced French series of 55 cases. *Eur. J. Clin. Microbiol. Infect. Dis.* 27: 37–43.
27. Ito, K., H. J. Bian, M. Molina, J. Han, J. Magram, E. Saar, C. Belunis, D. R. Bolin, R. Arceo, R. Campbell, et al. 1996. HLA-DR4-IE chimeric class II transgenic, murine class II-deficient mice are susceptible to experimental allergic encephalomyelitis. *J. Exp. Med.* 183: 2635–2644.
28. Chau, T. A., M. L. McCully, W. Brintnell, G. An, K. J. Kasper, E. D. Vinés, P. Kubes, S. M. Haeryfar, J. K. McCormick, E. Cairns, et al. 2009. Toll-like receptor 2 ligands on the staphylococcal cell wall downregulate SAg-induced T cell activation and prevent toxic shock syndrome. *Nat. Med.* 15: 641–648.
29. Hayworth, J. L., D. M. Mazzuca, S. Maleki Vareki, I. Welch, J. K. McCormick, and S. M. Haeryfar. 2012. CD1d-independent activation of mouse and human iNKT cells by bacterial SAgs. *Immunol. Cell Biol.* 90: 699–709.
30. Leder, L., A. Llera, P. M. Lavoie, M. I. Lebedeva, H. Li, R. P. Sékaly, G. A. Bohach, P. J. Gahr, P. M. Schlievert, K. Karjalainen, and R. A. Mariuzza. 1998. A mutational analysis of the binding of staphylococcal enterotoxins B and C3 to the T cell receptor beta chain and major histocompatibility complex class II. *J. Exp. Med.* 187: 823–833.
31. Pavlidis, P., and W. S. Noble. 2003. Matrix2png: a utility for visualizing matrix data. *Bioinformatics* 19: 295–296.
32. Howard, J. C., V. M. Varallo, D. C. Ross, J. H. Roth, K. J. Faber, B. Alman, and B. S. Gan. 2003. Elevated levels of beta-catenin and fibronectin in three-dimensional collagen cultures of Dupuytren's disease cells are regulated by tension in vitro. *BMC Musculoskelet. Disord.* 4: 16.
33. Sheridan, B. S., and L. Lefrancois. 2012. Isolation of mouse lymphocytes from small intestine tissues. *Curr. Protoc. Immunol.* 99: 3.19.1–3.19.11.

34. Mollick, J. A., M. Chintagumpala, R. G. Cook, and R. R. Rich. 1991. Staphylococcal exotoxin activation of T cells. Role of exotoxin-MHC class II binding affinity and class II isotype. *J. Immunol.* 146: 463–468.
35. DaSilva, L., B. C. Welcher, R. G. Ulrich, M. J. Aman, C. S. David, and S. Bavari. 2002. Humanlike immune response of human leukocyte antigen-DR3 transgenic mice to staphylococcal enterotoxins: a novel model for SAg vaccines. *J. Infect. Dis.* 185: 1754–1760.
36. Tilahun, A. Y., E. V. Marietta, T. T. Wu, R. Patel, C. S. David, and G. Rajagopalan. 2011. Human leukocyte antigen class II transgenic mouse model unmasks the significant extrahepatic pathology in toxic shock syndrome. *Am. J. Pathol.* 178: 2760–2773.
37. Roy, C. J., K. L. Warfield, B. C. Welcher, R. F. Gonzales, T. Larsen, J. Hanson, C. S. David, T. Krakauer, and S. Bavari. 2005. Human leukocyte antigen-DQ8 transgenic mice: a model to examine the toxicity of aerosolized staphylococcal enterotoxin B. *Infect. Immun.* 73: 2452–2460.
38. Hayworth, J. L., K. J. Kasper, M. Leon-Ponte, C. A. Herfst, D. Yue, W. C. Brintnell, D. M. Mazzuca, D. E. Heinrichs, E. Cairns, J. Madrenas, et al. 2009. Attenuation of massive cytokine response to the staphylococcal enterotoxin B SAg by the innate immunomodulatory protein lactoferrin. *Clin. Exp. Immunol.* 157: 60–70.
39. Szabo, P. A., A. Goswami, A. Memarnejadian, C. L. Mallett, P. J. Foster, J. K. McCormick, and S. M. Haeryfar. 2016. Swift intrahepatic accumulation of granulocytic myeloid-derived suppressor cells in a humanized mouse model of toxic shock syndrome. *J. Infect. Dis.* 213: 1990–1995.
40. Mueller, S. N., T. Gebhardt, F. R. Carbone, and W. R. Heath. 2013. Memory T cell subsets, migration patterns, and tissue residence. *Annu. Rev. Immunol.* 31: 137–161.
41. Michel, M. L., A. C. Keller, C. Paget, M. Fujio, F. Trottein, P. B. Savage, C. H. Wong, E. Schneider, M. Dy, and M. C. Leite-de-Moraes. 2007. Identification of an IL-17-producing NK1.1(neg) iNKT cell population involved in airway neutrophilia. *J. Exp. Med.* 204: 995–1001.
42. Ivanov, I. I., B. S. McKenzie, L. Zhou, C. E. Tadokoro, A. Lepelley, J. J. Lafaille, D. J. Cua, and D. R. Littman. 2006. The orphan nuclear receptor RORgammat directs the differentiation program of proinflammatory IL-17+ T helper cells. *Cell* 126: 1121–1133.
43. Kum, W. W., S. B. Cameron, R. W. Hung, S. Kalyan, and A. W. Chow. 2001. Temporal sequence and kinetics of proinflammatory and anti-inflammatory cytokine secretion induced by toxic shock syndrome toxin 1 in human peripheral blood mononuclear cells. *Infect. Immun.* 69: 7544–7549.
44. Tilahun, A. Y., M. Holz, T. T. Wu, C. S. David, and G. Rajagopalan. 2011. Interferon gamma-dependent intestinal pathology contributes to the lethality in bacterial SAg-induced toxic shock syndrome. *PLoS One* 6: e16764.
45. Chen, C. Y., N. Ezzeddine, and A. B. Shyu. 2008. Messenger RNA half-life measurements in mammalian cells. *Methods Enzymol.* 448: 335–357.
46. Sallusto, F., D. Lenig, R. Förster, M. Lipp, and A. Lanzavecchia. 1999. Two subsets of memory T lymphocytes with distinct homing potentials and effector functions. *Nature* 401: 708–712.
47. Annunziato, F., L. Cosmi, V. Santarlasci, L. Maggi, F. Liotta, B. Mazzinghi, E. Parente, L. Filì, S. Ferri, F. Frosali, et al. 2007. Phenotypic and functional features of human Th17 cells. *J. Exp. Med.* 204: 1849–1861.
48. Singh, S. P., H. H. Zhang, J. F. Foley, M. N. Hedrick, and J. M. Farber. 2008. Human T cells that are able to produce IL-17 express the chemokine receptor CCR6. *J. Immunol.* 180: 214–221.
49. Liu, H., and C. Rohowsky-Kochan. 2008. Regulation of IL-17 in human CCR6+ effector memory T cells. *J. Immunol.* 180: 7948–7957.
50. Gao, Y., and A. P. Williams. 2015. Role of innate T cells in anti-bacterial immunity. *Front. Immunol.* 6: 302.
51. McArthur, M. A., and M. B. Sztein. 2013. Unexpected heterogeneity of multifunctional T cells in response to SAg stimulation in humans. *Clin. Immunol.* 146: 140–152.
52. Onishi, R. M., and S. L. Gaffen. 2010. Interleukin-17 and its target genes: mechanisms of interleukin-17 function in disease. *Immunology* 129: 311–321.
53. Iwakura, Y., H. Ishigame, S. Saijo, and S. Nakae. 2011. Functional specialization of interleukin-17 family members. *Immunity* 34: 149–162.
54. Zrioual, S., M. L. Toh, A. Tournadre, Y. Zhou, M. A. Cazalis, A. Pachot, V. Miossec, and P. Miossec. 2008. IL-17RA and IL-17RC receptors are essential for IL-17A-induced ELR+ CXC chemokine expression in synoviocytes and are overexpressed in rheumatoid blood. *J. Immunol.* 180: 655–663.
55. Shahrara, S., S. R. Pickens, A. Dorfleutner, and R. M. Pope. 2009. IL-17 induces monocyte migration in rheumatoid arthritis. *J. Immunol.* 182: 3884–3891.
56. Ko, C. Y., W. C. Chang, and J. M. Wang. 2015. Biological roles of CCAAT/Enhancer-binding protein delta during inflammation. *J. Biomed. Sci.* 22: 6.
57. Fromenty, B., and D. Pessayre. 1995. Inhibition of mitochondrial beta-oxidation as a mechanism of hepatotoxicity. *Pharmacol. Ther.* 67: 101–154.
58. Cho, J. S., E. M. Pietras, N. C. Garcia, R. I. Ramos, D. M. Farzam, H. R. Monroe, J. E. Magorien, A. Blauvelt, J. K. Kolls, A. L. Cheung, et al. 2010. IL-17 is essential for host defense against cutaneous *Staphylococcus aureus* infection in mice. *J. Clin. Invest.* 120: 1762–1773.
59. Wang, B., T. Dileepan, S. Briscoe, K. A. Hyland, J. Kang, A. Khoruts, and P. P. Cleary. 2010. Induction of TGF-beta1 and TGF-beta1-dependent predominant Th17 differentiation by group A streptococcal infection. *Proc. Natl. Acad. Sci. USA* 107: 5937–5942.
60. Miethke, T., C. Wahl, K. Heeg, B. Echtenacher, P. H. Krammer, and H. Wagner. 1992. T cell-mediated lethal shock triggered in mice by the SAg staphylococcal enterotoxin B: critical role of tumor necrosis factor. *J. Exp. Med.* 175: 91–98.
61. Stiles, B. G., S. Bavari, T. Krakauer, and R. G. Ulrich. 1993. Toxicity of staphylococcal enterotoxins potentiated by lipopolysaccharide: major histocompatibility complex class II molecule dependency and cytokine release. *Infect. Immun.* 61: 5333–5338.
62. Leist, M., F. Gantner, I. Bohlinger, G. Tiegs, P. G. Germann, and A. Wendel. 1995. Tumor necrosis factor-induced hepatocyte apoptosis precedes liver failure in experimental murine shock models. *Am. J. Pathol.* 146: 1220–1234.
63. Mignon, A., N. Rouquet, M. Fabre, S. Martin, J. C. Pagès, J. F. Dhainaut, A. Kahn, P. Briand, and V. Joulin. 1999. LPS challenge in D-galactosamine-sensitized mice accounts for caspase-dependent fulminant hepatitis, not for septic shock. *Am. J. Respir. Crit. Care Med.* 159: 1308–1315.
64. Wang, H., and S. Ma. 2008. The cytokine storm and factors determining the sequence and severity of organ dysfunction in multiple organ dysfunction syndrome. *Am. J. Emerg. Med.* 26: 711–715.
65. Tilahun, A. Y., V. R. Chowdhary, C. S. David, and G. Rajagopalan. 2014. Systemic inflammatory response elicited by SAg destabilizes T regulatory cells, rendering them ineffective during toxic shock syndrome. *J. Immunol.* 193: 2919–2930.
66. Islander, U., A. Andersson, E. Lindberg, I. Adlerberth, A. E. Wold, and A. Rudin. 2010. Superantigenic *Staphylococcus aureus* stimulates production of interleukin-17 from memory but not naive T cells. *Infect. Immun.* 78: 381–386.
67. Niebuhr, M., M. Gathmann, H. Scharonow, D. Mamerow, S. Mommert, H. Balaji, and T. Werfel. 2011. Staphylococcal alpha-toxin is a strong inducer of interleukin-17 in humans. *Infect. Immun.* 79: 1615–1622.
68. Esplugues, E., S. Huber, N. Gagliani, A. E. Hauser, T. Town, Y. Y. Wan, W. O'Connor, Jr., A. Rongvaux, N. Van Rooijen, A. M. Haberman, et al. 2011. Control of TH17 cells occurs in the small intestine. *Nature* 475: 514–518.
69. Hirota, K., J. H. Duarte, M. Veldhoen, E. Hornsby, Y. Li, D. J. Cua, H. Ahlfors, C. Wilhelm, M. Tolaini, U. Menzel, et al. 2011. Fate mapping of IL-17-producing T cells in inflammatory responses. *Nat. Immunol.* 12: 255–263.
70. Sheridan, B. S., and L. Lefrançois. 2011. Regional and mucosal memory T cells. *Nat. Immunol.* 12: 485–491.
71. Danielsen, E. M., G. H. Hansen, and E. Karlsdóttir. 2013. *Staphylococcus aureus* enterotoxins A- and B: binding to the enterocyte brush border and uptake by perturbation of the apical endocytic membrane traffic. *Histochem. Cell Biol.* 139: 513–524.
72. Krakauer, T., M. J. Buckley, and D. Fisher. 2010. Proinflammatory mediators of toxic shock and their correlation to lethality. *Mediators Inflamm.* 2010: 517594.
73. Faulkner, L., A. Cooper, C. Fantino, D. M. Altmann, and S. Sriskandan. 2005. The mechanism of SAg-mediated toxic shock: not a simple Th1 cytokine storm. *J. Immunol.* 175: 6870–6877.
74. Chen, J., J. Cascio, J. D. Magee, P. Techasintana, M. M. Gubin, G. M. Dahm, R. Calaluce, S. Yu, and U. Atasoy. 2013. Posttranscriptional gene regulation of IL-17 by the RNA-binding protein HuR is required for initiation of experimental autoimmune encephalomyelitis. *J. Immunol.* 191: 5441–5450.
75. Lee, H. H., N. A. Yoon, M. T. Vo, C. W. Kim, J. M. Woo, H. J. Cha, Y. W. Cho, B. J. Lee, W. J. Cho, and J. W. Park. 2012. Tristetraprolin down-regulates IL-17 through mRNA destabilization. *FEBS Lett.* 586: 41–46.
76. Khan, D., and S. Ansar Ahmed. 2015. Regulation of IL-17 in autoimmune diseases by transcriptional factors and microRNAs. *Front. Genet.* 6: 236.
77. Pepper, M., and M. K. Jenkins. 2011. Origins of CD4(+) effector and central memory T cells. *Nat. Immunol.* 12: 467–471.
78. Muranski, P., Z. A. Borman, S. P. Kerkar, C. A. Klebanoff, Y. Ji, L. Sanchez-Perez, M. Sukumar, R. N. Reger, Z. Yu, S. J. Kern, et al. 2011. Th17 cells are long lived and retain a stem cell-like molecular signature. *Immunity* 35: 972–985.
79. Kryczek, I., E. Zhao, Y. Liu, Y. Wang, L. Vatan, W. Szeliga, J. Moyer, A. Klimczak, A. Lange, and W. Zou. 2011. Human TH17 cells are long-lived effector memory cells. *Sci. Transl. Med.* 3: 104ra100.
80. Björkander, S., L. Hell, M. A. Johansson, M. M. Forsberg, G. Lasaviciute, S. Roos, U. Holmlund, and E. Sverremark-Ekström. 2016. Staphylococcus aureus-derived factors induce IL-10, IFN-γ and IL-17A-expressing FOXP3+CD161+ T-helper cells in a partly monocyte-dependent manner. *Sci. Rep.* 6: 22083.
81. Taylor, A. L., and M. J. Llewelyn. 2010. Superantigen-induced proliferation of human CD4+CD25- T cells is followed by a switch to a functional regulatory phenotype. *J. Immunol.* 185: 6591–6598.
82. Azuma, K., K. Koike, T. Kobayashi, T. Mochizuki, K. Mashiko, and Y. Yamamoto. 2004. Detection of circulating SAgs in an intensive care unit population. *Int. J. Infect. Dis.* 8: 292–298.
83. Prindeze, N. J., B. M. Amundsen, A. R. Pavlovich, D. W. Paul, B. C. Carney, L. T. Moffatt, and J. W. Shupp. 2014. Staphylococcal SAgs and toxins are detectable in the serum of adult burn patients. *Diagn. Microbiol. Infect. Dis.* 79: 303–307.
84. Sriskandan, S., D. Moyes, and J. Cohen. 1996. Detection of circulating bacterial SAg and lymphotoxin-alpha in patients with streptococcal toxic-shock syndrome. *Lancet* 348: 1315–1316.
85. Russell, C. B., H. Rand, J. Bigler, K. Kerkof, M. Timour, E. Bautista, J. G. Krueger, D. H. Salinger, A. A. Welcher, and D. A. Martin. 2014. Gene expression profiles normalized in psoriatic skin by treatment with brodalumab, a human anti-IL-17 receptor monoclonal antibody. *J. Immunol.* 192: 3828–3836.

86. Crowe, C. R., K. Chen, D. A. Pociask, J. F. Alcorn, C. Krivich, R. I. Enelow, T. M. Ross, J. L. Witztum, and J. K. Kolls. 2009. Critical role of IL-17RA in immunopathology of influenza infection. *J. Immunol.* 183: 5301–5310.
87. Cone, L. A., D. R. Woodard, P. M. Schlievert, and G. S. Tomory. 1987. Clinical and bacteriologic observations of a toxic shock-like syndrome due to *Streptococcus pyogenes. N. Engl. J. Med.* 317: 146–149.
88. Van Lierde, S., W. J. van Leeuwen, J. Ceuppens, L. Cornette, P. Goubau, and J. Van Eldere. 1997. Toxic shock syndrome without rash in a young child: link with syndrome of hemorrhagic shock and encephalopathy? *J. Pediatr.* 131: 130–134.
89. Koskinas, J., I. P. Gomatos, D. G. Tiniakos, N. Memos, M. Boutsikou, A. Garatzioti, A. Archimandritis, and A. Betrosian. 2008. Liver histology in ICU patients dying from sepsis: a clinico-pathological study. *World J. Gastroenterol.* 14: 1389–1393.
90. DeVries, A. S., L. Lesher, P. M. Schlievert, T. Rogers, L. G. Villaume, R. Danila, and R. Lynfield. 2011. Staphylococcal toxic shock syndrome 2000-2006: epidemiology, clinical features, and molecular characteristics. *PLoS One* 6: e22997.
91. Low, D. E. 2013. Toxic shock syndrome: major advances in pathogenesis, but not treatment. *Crit. Care Clin.* 29: 651–675.
92. Linnér, A., J. Darenberg, J. Sjölin, B. Henriques-Normark, and A. Norrby-Teglund. 2014. Clinical efficacy of polyspecific intravenous immunoglobulin therapy in patients with streptococcal toxic shock syndrome: a comparative observational study. *Clin. Infect. Dis.* 59: 851–857.

Target (reference if applicable)	Reactivity	Sequence (5'-3') or Accession #	Source
HLA-DRA-IEα Forward (27)	Human	GGGAAGCAGGGGGACTATGAC	Sigma-Aldrich
HLA-DRA-IEα Reverse (27)	Human	TTAGGGCAATGACTTCGTAGG	Sigma-Aldrich
HLA-DRB1*0401-IEβ Forward (27)	Human	TGAAAGCGGTGCGTGCTGTTTAA	Sigma-Aldrich
HLA-DRB1*0401-IEβ Reverse (27)	Human	CACCCGCTCCGTCCCGTTGAA	Sigma-Aldrich
HLA-DR Transgene Insertion Site Forward*	Mouse	CCATGGACAAGGCAGGGACAAA	Sigma-Aldrich
HLA-DR Transgene Insertion Site Reverse*	Mouse	CCGTGACCAAAATGCACATTGAA	Sigma-Aldrich
IL-17A-GFP Common Forward (Jackson Primer #15240)	Mouse	AAGCTGGACCACCACATGA	Sigma-Aldrich
IL-17A-GFP Wildtype Reverse (Jackson Primer #15241)	Mouse	TGAATCCACATTCCTTGCTG	Sigma-Aldrich
IL-17A-GFP Mutant Reverse (Jackson Primer #11188)	Mouse	GACATTCAACAGACCTTGCATTC	Sigma-Aldrich
IAβ-neo^r Forward	Mouse	GGGAGGAGTACGTGCGCTACGACAG	Sigma-Aldrich
IAβ-neo^r Reverse	Mouse	GAGAACCTGCGTGCAATCCATCTTG	Sigma-Aldrich
IAβ Forward	Mouse	GGCATTTCGTGTACCAGTTCATGG	Sigma-Aldrich
IAβ Reverse	Mouse	GTCTCCGGCCCCTCGTAGTTGTGT	Sigma-Aldrich
CCL11	Human	Hs00237013_m1	Thermo Fischer
CCL2	Human	Hs00234140_m1	Thermo Fischer
CCL20	Human	Hs00355476_m1	Thermo Fischer
CCL5	Human	Hs00982282_m1	Thermo Fischer
CCL7	Human	Hs00171147_m1	Thermo Fischer
CEBPB	Human	Hs00270923_s1	Thermo Fischer
CEBPD	Human	Hs00270931_s1	Thermo Fischer
CSF2	Human	Hs00929873_m1	Thermo Fischer
CSF3	Human	Hs00738432_g1	Thermo Fischer
CXCL1	Human	Hs00605382_gH	Thermo Fischer
CXCL10	Human	Hs01124252_g1	Thermo Fischer
CXCL11	Human	Hs04187682_g1	Thermo Fischer
CXCL12	Human	Hs03676656_mH	Thermo Fischer
CXCL2	Human	Hs00601975_m1	Thermo Fischer
CXCL5	Human	Hs01099660_g1	Thermo Fischer
CXCL6	Human	Hs00605742_g1	Thermo Fischer
CXCL9	Human	Hs00171065_m1	Thermo Fischer
GATA3	Human	Hs00231122_m1	Thermo Fischer
IFNG	Human	Hs00989291_m1	Thermo Fischer
IL10	Human	Hs00961622_m1	Thermo Fischer
IL12A	Human	Hs01073447_m1	Thermo Fischer
IL12B	Human	Hs01011518_m1	Thermo Fischer
IL13	Human	Hs00174379_m1	Thermo Fischer
IL17A	Human	Hs00174383_m1	Thermo Fischer
IL17F	Human	Hs00369400_m1	Thermo Fischer
IL18	Human	Hs01038788_m1	Thermo Fischer
IL19	Human	Hs00604657_m1	Thermo Fischer
IL1B	Human	Hs00174097_m1	Thermo Fischer
IL2	Human	Hs00174114_m1	Thermo Fischer
IL22	Human	Hs01574154_m1	Thermo Fischer
IL23A	Human	Hs00900828_g1	Thermo Fischer
IL4	Human	Hs00174122_m1	Thermo Fischer
IL6	Human	Hs00985639_m1	Thermo Fischer
IL8	Human	Hs00174103_m1	Thermo Fischer
LTA	Human	Hs04188773_g1	Thermo Fischer
MYD88	Human	Hs01573837_g1	Thermo Fischer
NFKB1	Human	Hs00765730_m1	Thermo Fischer
NFKBIZ	Human	Hs00230071_m1	Thermo Fischer
NOS2	Human	Hs01075529_m1	Thermo Fischer
PTGS2	Human	Hs00153133_m1	Thermo Fischer
RORC	Human	Hs01076112_m1	Thermo Fischer
RPL13A	Human	Hs04194366_g1	Thermo Fischer
TBP	Human	Hs00427620_m1	Thermo Fischer
TBX21	Human	Hs00203436_m1	Thermo Fischer
TGFB1	Human	Hs00998133_m1	Thermo Fischer
TNFA	Human	Hs01113624_g1	Thermo Fischer
ZBTB16	Human	Hs00957433_m1	Thermo Fischer

Supplemental Table 1: PCR primers/probes used in this study. *Primer was designed to span the insertion site of the HLA-DR4 transgenes in the mouse genome (Raffegerst *et al*: PLoS ONE 2009, 4(12): e8539), thus enabling discrimination between homozygous and heterozygous transgenic mice.

Target	Reactivity	Host Species	Clone/ Accession #	Isotype	Fluorochrome	Source
Surface Molecules						
TCRβ	Mouse	Arm. Hamster	H57-597	IgG	PE-Cyanine7	eBioscience
CD4	Mouse	Rat	GK1.5	IgG2b, κ	Alexa Fluor® 700	eBioscience
CD44	Human/ Mouse	Rat	IM7	IgG2b, κ	PerCP-Cyanine5.5	eBioscience
CD62L	Mouse	Rat	MEL-14	IgG2a, κ	APC-eFluor® 780	eBioscience
CCR7	Mouse	Rat	4B12	IgG2a, κ	APC	eBioscience
CD127	Mouse	Rat	A7R34	IgG2a, κ	PE	eBioscience
*i*NKT TCR (detected by CD1d loaded tetramer)	Mouse	Mouse	N/A	N/A	APC	NIH Tetramer Core Facility
CD3ε	Human	Mouse	OKT3 UCHT1	IgG2a, κ IgG1, κ	FITC eFluor® 450	eBioscience eBioscience
CD4	Human	Mouse	RPA-T4 SK3	IgG1, κ IgG1, κ	Alexa Fluor® 700 Brilliant Violet™ 510	eBioscience BD Biosciences
CD8	Human	Mouse	RPA-T8	IgG1, κ	Alexa Fluor® 700	eBioscience
CD45RA	Human	Mouse	HI100	IgG2b, κ	PE PE-Cyanine7	eBioscience eBioscience
CD45RO	Human	Mouse	UCHL1	IgG2a, κ	APC Brilliant Violet™ 785	eBioscience BD Biosciences
CCR6	Human	Mouse	G034E3	IgG2b, κ	PE	BioLegend
CCR7	Human	Rat	3D12	IgG2a, κ	PerCP-eFluor® 710 PE-eFluor® 610	eBioscience eBioscience
CD161	Human	Mouse	HP-3G10	IgG1	APC PerCP-Cyanine5.5	eBioscience eBioscience
Vα7.2 TCR	Human	Mouse	3C10	IgG1, κ	PE PerCP-Cyanine5.5	BioLegend BioLegend
*i*NKT TCR (detected by CD1d loaded tetramer)	Human	Human	N/A	N/A	APC	NIH Tetramer Core Facility
γδ TCR	Human	Mouse	B1 B1.1	IgG1, κ IgG1, κ	PE PerCP-eFluor® 710	BD Biosciences eBioscience
Cytokines						
IL-17A	Human	Mouse	eBio64-DEC17	IgG1, κ	PE PE-Cyanine7	eBioscience eBioscience
IFNγ	Human	Mouse	4S.B3	IgG1, κ	PE PE-Cyanine7	eBioscience eBioscience
Transcription Factors						
RORγT	Human	Mouse	Q21-559	IgG2a, κ	Alexa Fluor® 647	BD Biosciences
FoxP3	Human	Mouse	236A/E7	IgG1, κ	APC	eBioscience
Prime-Flow RNA						
IL-17A	Human		NM_002190		Type 1 Alexa Fluor® 647	Affymetrix
IFNγ	Human		NM_000619		Type 4 Alexa Fluor® 488	Affymetrix
RPL13A	Human		NM_012423		Type 6 Alexa Fluor® 750	Affymetrix

Supplemental Table 2: Antibodies/tetramers used in this study

Target	Fold Change (SEB relative to medium control)		
	Donor 1	Donor 2	Donor 3
IL22	1059.25	355.71	2198.29
IL17F	737.24	137.67	780.40
IFNG	304.81	661.94	445.69
IL17A	253.73	96.47	651.44
CSF3	583.76	20.88	296.10
IL6	111.03	6.77	140.41
IL19	70.28	50.68	115.96
IL13	45.96	24.00	84.64
IL2	32.45	58.60	19.38
IL12B	32.24	2.08	71.23
CCL20	40.69	2.49	45.23
CSF2	17.49	26.89	21.14
IL10	28.65	5.74	29.33
CXCL9	2.59	37.62	4.11
CXCL1	10.29	0.74	31.46
PTGS2	14.72	1.86	12.92
LTA	5.37	13.70	10.01
CXCL11	0.51	14.43	1.33
IL1B	6.39	1.20	5.01
TNFA	2.26	3.47	6.43
CXCL5	3.93	0.19	7.15
CXCL2	4.29	0.56	5.42
TBX21	3.48	3.80	0.95
IL8	3.98	0.82	3.03
IL12A	2.12	3.13	1.63
IL4	3.13	1.22	2.53
IL23A	2.13	2.12	2.20
NFKB1	2.43	1.53	2.02
CXCL6	2.75	0.08	3.14
NFKBIZ	2.11	1.29	1.74
CCL2	1.86	0.39	2.68
RORC	1.87	2.01	1.00
CXCL10	0.33	3.50	0.61
CEBPB	1.11	0.89	0.90
ZBTB16	0.93	1.05	0.73
TGFB1	0.70	1.06	0.66
GATA3	0.50	0.66	0.82
CCL7	0.55	0.26	1.00
CCL5	0.68	0.60	0.34
MYD88	0.58	0.63	0.32
NOS2	0.58	0.12	0.36
CEBPD	0.23	0.33	0.32
CXCL12	0.14	0.27	0.15
IL18	0.12	0.16	0.06

Supplemental Table 3: Fold changes in gene expression of SEB-stimulated human PBMCs relative to medium control.

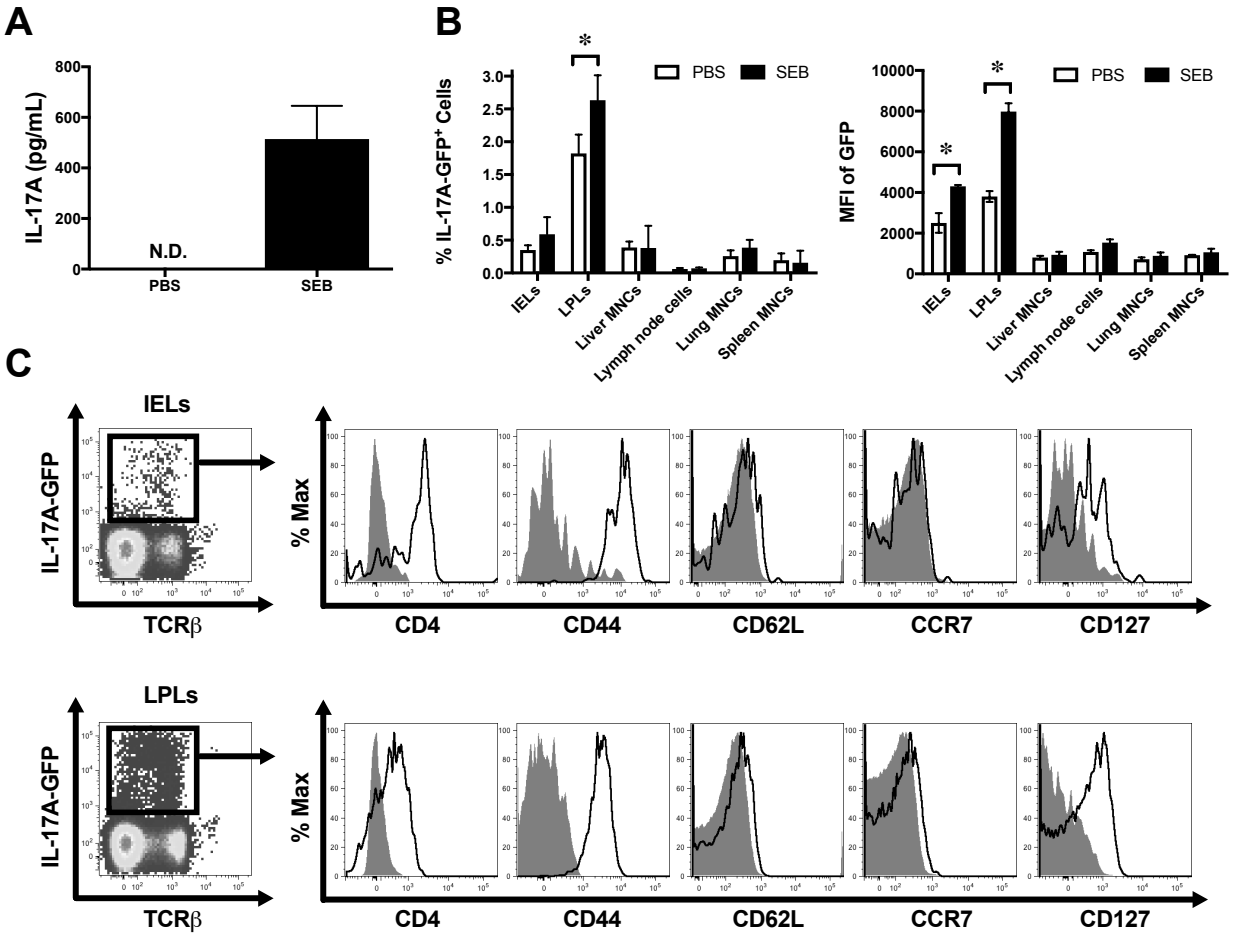

Supplemental Fig. 1: SEB-primed D17 mice launch a rapid IL-17A response and harbor an enriched population of IL-17A-producing CD4$^+$ T_{EM} cells in their small intestine. D17 mice, generated by crossing DR4tg and IL-17A-GFP reporter mice, were injected *i.p.* with 50 μg SEB or with PBS. (**A**) Two hours later, mice were euthanized and the IL-17A content of serum samples was measured. N.D.: not detectable. Error bars represent SEM (n=3/group). (**B**) The frequencies of GFP$^+$ cells and the MFI of GFP were determined in non-parenchymal mononuclear cells (MNCs) from indicated tissues and among intestinal intraepithelial lymphocytes (IELs) and lamina propria lymphocytes (LPLs). * denotes $p \leq 0.05$ by two-tailed Student's *t*-test. (**C**) GFP$^+$ IELs and LPLs from SEB-injected mice were immunophenotyped using fluorochrome-labeled mAbs to indicated markers (open histograms) and isotype controls (filled histograms). Depicted data represent findings from 3 mice used in independent experiments.